

AD A113606

AFWAL-TR-82-4004



PROPERTIES OF ORGANIC MATRIX SHORT FIBER COMPOSITES

GEORGE S. SPRINGER

DEPARTMENT OF MECHANICAL ENGINEERING AND APPLIED MECHANICS
THE UNIVERSITY OF MICHIGAN
ANN ARBOR, MICHIGAN 48109

FEBRUARY 1982

FINAL REPORT FOR PERIOD OCTOBER 1981-DECEMBER 1981

Approved for Public Release; Distribution Unlimited

MATERIALS LABORATORY
AIR FORCE WRIGHT AERONAUTICAL LABORATORIES
AIR FORCE SYSTEMS COMMAND
WRIGHT-PATTERSON AFB, OHIO 45433

DTIC FILE COPY

DTIC
ELECTE
APR 20 1982
H

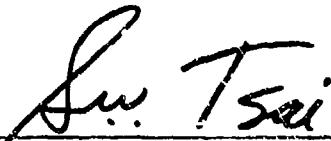
82 04 20 005

NOTICE

When Government drawings, specifications, or other data are used for any purpose other than in connection with a definitely related Government procurement operation, the United States Government thereby incurs no responsibility nor any obligation whatsoever; and the fact that the Government may have formulated, furnished, or in any way supplied the said drawings, specifications, or other data, is not to be regarded by implication or otherwise as in any manner licensing the holder or any other person or corporation, or conveying any rights or permission to manufacture, use, or sell any patented invention that may in any way be related thereto.

This report has been reviewed by the Office of Public Affairs (ASD/PA) and is releasable to the National Technical Information Service (NTIS). At NTIS, it will be available to the general public, including foreign nations.

This technical report has been reviewed and is approved for publication.



S. W. TSAI, Project Engineer & Chief
Mechanics and Surface Interactions Branch
Nonmetallic Materials Division

FOR THE COMMANDER



F. D. CHERRY, Chief
Nonmetallic Materials Division

"If your address has changed, if you wish to be removed from our mailing list, or if the addressee is no longer employed by your organization please notify AFWAL/MLBM, W-PAFB, Ohio 45433 to help us maintain a current mailing list.

Copies of this report should not be returned unless return is required by security considerations, contractual obligations, or notice on a specific document.

REPORT DOCUMENTATION PAGE		READ INSTRUCTIONS BEFORE COMPLETING FORM
1. REPORT NUMBER AFWAL-TR-82-4004	2. GOVT ACCESSION NO. AD A113 606	3. RECIPIENT'S CATALOG NUMBER
4. TITLE (and Subtitle) PROPERTIES OF ORGANIC MATRIX SHORT FIBER COMPOSITES		5. TYPE OF REPORT & PERIOD COVERED October, 1981-December 1981
		6. PERFORMING ORG. REPORT NUMBER
7. AUTHOR(s) George S. Springer		8. CONTRACT OR GRANT NUMBER(s) F33615-81-C-5050 F33615-79-C-5082
9. PERFORMING ORGANIZATION NAME AND ADDRESS Department of Mechanical Engineering and Applied Mechanics, The University of Michigan Ann Arbor, Michigan 48109		10. PROGRAM ELEMENT, PROJECT, TASK AREA & WORK UNIT NUMBERS 2307P113 M-332-68
11. CONTROLLING OFFICE NAME AND ADDRESS Materials Laboratory (AFWAL/MLBM) Air Force Wright Aeronautical Laboratories Wright-Patterson, AFB, OH 45433		12. REPORT DATE February 1982
14. MONITORING AGENCY NAME & ADDRESS (if different from Controlling Office)		13. NUMBER OF PAGES 77
		15. SECURITY CLASS. (of this report) Unclassified
		15a. DECLASSIFICATION/DOWNGRADING SCHEDULE
16. DISTRIBUTION STATEMENT (of this Report) Approved for public release, distribution unlimited		
17. DISTRIBUTION STATEMENT (of the abstract entered in Block 20, if different from Report)		
18. SUPPLEMENTARY NOTES		
19. KEY WORDS (Continue on reverse side if necessary and identify by block number) Composite Materials Short Fiber Composites Sheet Molding Compounds		
20. ABSTRACT (Continue on reverse side if necessary and identify by block number) In this report, a summary is given of the engineering properties of chopped fiber reinforced sheet molding compounds and of the effects of service environment on these properties. The properties surveyed include tensile strength and modulus, compression strength and modulus, shear strength and modulus, flexural strength and modulus, notch sensitivity, fatigue, creep, vibration damping, response to dynamic impact, moisture absorption characteristics and thermal expansion. The basic properties of adhesive bonded single		

CONFIDENTIAL
SECURITY CLASSIFICATION OF THIS PAGE(When Data Entered)

lap joints are also included in this survey.

28
SECURITY CLASSIFICATION OF THIS PAGE(When Data Entered)

FOREWORD

This report was prepared by George S. Springer, Department of Mechanical Engineering and Applied Mechanics, The University of Michigan for the Mechanics and Surface Interactions Branch (AFWAL/MLBM), Nonmetallic Materials Division, Materials Laboratory, Air Force Wright Aeronautical Laboratories, Wright-Patterson AFB, Ohio. The work was performed under a Subcontract with the Universal Technology Corporation, Contract Number F 33615-79-C-5082, Project number M-332-68.

This report covers work accomplished during the period October, 1981-December 1981.



Accession For	
NTIS GRA&I	<input checked="" type="checkbox"/>
DTIC TAB	<input type="checkbox"/>
Unannounced	<input type="checkbox"/>
Justification	
By _____	
Distribution/	
Availability Codes	
Dist	Avail and/or Special
<div style="text-align: center;"> </div>	

TABLE OF CONTENTS

<u>SECTION</u>		<u>PAGE</u>
I	INTRODUCTION	1
II	MATERIALS AND PROCESSING	2
III	STATIC PROPERTIES	3
	1. Tensile Strength and Modulus	3
	2. Compression Strength and Modulus	3
	3. Shear Strength and Shear Modulus	4
	4. Flexural Strength and Modulus	4
	5. Notch Sensitivity	4
IV	FATIGUE	5
V	CREEP	7
VI	ADHESIVE BONDED SINGLE LAP JOINTS	7
	1. Moisture Absorption Characteristics	7
	2. Lap Shear Strength	8
	3. Fatigue	9
	4. Creep	9
VII	VIBRATION DAMPING	10
VIII	DYNAMIC IMPACT	11
IX	MOISTURE ABSORPTION	12
X	THERMAL EXPANSION	13
XI	CONCLUDING REMARKS	14
	REFERENCES	15

LIST OF ILLUSTRATIONS

<u>FIGURE</u>		<u>PAGE</u>
1	The use of plastics in passenger cars (ref. 1).	35
2	Illustration of glass fiber reinforced sheet molding compounds	36
3	Schematic of process used to manufacture glass fiber reinforced SMC composites (Owens Corning Fiberglas System)	37
4	Schematic of process used to manufacture XMC composites (PPG Industries System)	38
5	Schematic of compression molding of SMC composites . .	39
6	The effect of fiber orientation on the tensile strength and tensile modulus of XMC-3 and SMC-C20/R30 composites (ref. 3)	40
7	The effect of the amount of chopped fibers on the tensile strength of XMC-3 composites. Total fiber content by weight = 75 percent (ref. 7)	41
8	The effect of temperature on the tensile strength and tensile modulus. (L - longitudinal, T - transverse direction) (refs. 2, 3, 5)	42
9	The effect of temperature on the compression strength and compression modulus. (L - longitudinal, T - transverse direction) (ref. 3)	43
10	The effect of temperature on the flexural strength and flexural modulus. (L - longitudinal, T - transverse direction) (ref. 3)	44
11	The effect of the amount of chopped fibers on the flexural strength and flexural modulus of XMC-3 composites. Total fiber content by weight = 75 percent (ref. 7) . .	45
12	Changes in tensile strengths due to different diameter circular holes ("notches") (ref. 3)	46
13	Typical result of fatigue test and definition of symbols used in the presentation of the fatigue results	47
14	Tension-tension fatigue results. R = 0.05 (except for VE-SMC-R50 and VE-SMC-R-65) (refs. 2, 5, 6)	48

LIST OF ILLUSTRATIONS (Continued)

<u>FIGURE</u>		<u>PAGE</u>
15	Tension-tension fatigue results. $R = 0.05$ (ref. 3) . .	49
16	Tension-tension fatigue results. $R = 0.05$ (ref. 2) . .	50
17	Compression-tension fatigue results. $R = -1$ (ref. 2) .	51
18	Flexural fatigue results. (ref. 2)	52
19	Creep strain ($\epsilon_N - \epsilon_0$) during tension-tension fatigue tests as functions of load (percent of ultimate tensile strength). $R = 0.05$ (refs. 2, 3)	53
20	Modulus decay during tension-tension fatigue tests as a function of load (percent of ultimate tensile strength) $R = 0.05$ (ref. 3).	54
21	Modulus decay during tension-tension fatigue tests as a function of load (percent of ultimate tensile strength). $R = 0.05$ (refs. 2, 4)	55
22	Creep of XMC-3 at 70, 50 and 30 percent of static ultimate tensile strength (L - longitudinal, T - transverse direction) (ref. 3)	56
23	Creep of SMC-C20/R30 at 70, 50 and 30 percent of static ultimate tensile strength. (L - longitudinal, T - transverse direction) (ref. 3)	57
24	Creep of SMC-R25 under different loads (percent of static ultimate tensile strength) (ref. 2)	58
25	Creep of SMC-R50 and VE-SMC-R50 under different loads (percent of static ultimate tensile strength) (refs. 5, 6).	59
26	Strain (elongation) of SMC-R50 at failure as a function of temperature (ref. 5)	60
27	Creep of SMC-R57 under different loads (percent of static ultimate tensile strength) (ref. 2)	61
28	Creep of SMC-R65 under different loads (percent of static ultimate tensile strength)	62

LIST OF ILLUSTRATIONS (Concluded)

<u>FIGURE</u>		<u>PAGE</u>
29	Moisture absorption of adhesive bonded XMC-3 to SMC-R50 single lap joints	63
30	Maximum shear stress of adhesive bonded single lap joints (SMC-R50 to SMC-R50 and SMC-R25 to SMC-R25) during tension-tension fatigue (ref. 11)	64
31	Creep of adhesive bonded single lap joints (SMC-R50 to SMC-R50 and XMC-3 to SMC-R50) immersed in air water, and 5% NaCl-water mixture under different loads (percent of static ultimate tensile strength	65
32	Creep of adhesive bonded single lap joints (SMC-R50 to SMC-R50 and SMC-R25 to SMC-R25) during tension-tension fatigue under different loads (-30% UTS, ---50% UTS, --70% UTS) (ref. 11)	66
33	Energy absorbed by different materials during impact against a fixed barrier. Impact speed 24 km/h (ref. 13)	67
34	Typical output of impact test using Rheometrics impact tester (ref. 3)	68
35	Weight change during immersion in humid air and in saturated salt water (ref. 4)	69
36	Weight change during immersion in different types of hydrocarbons (refs. 4, 14)	70
37	Weight change of XMC-3 immersed in humid air, water, and in 5% NaCl-water mixture (ref. 4)	71

LIST OF TABLES

<u>TABLE</u>		<u>PAGE</u>
1	Material formulations and densities of SMC materials (PPG-PPG Industries, OFC-Owens Corning Fiberglas) (refs. 2,3)	17
2	VE-SMC-R50 past formulation	18
3	Room temperature ultimate tensile strength (S_t), tensile modulus (E_t), tensile failure strain (ϵ_t), and Poisson's ratio (ν_t) (L - longitudinal, T - transverse direction) (refs. 2-6)	19
4	Tensile strength retained (percent) after immersion in different fluids for 30 and 180 days. (L - longitudinal, T - transverse direction) (refs. 3, 4).	20
5	Tensile modulus retained (percent) after immersion in different fluids for 30 and 180 days (ref. 4)	21
6	Room temperature compression strength (S_c), compression modulus (E_c) and compression failure strain (ϵ_c) (L - longitudinal, T - transverse direction) (refs. 2, 3).	22
7	Room temperature in plane shear strength (S_{LT}), in plane shear modulus (E_{LT}), short beam shear strength (S_s), and short beam shear modulus (G_s) (refs. 3, 4, 8)	23
8	Losses in in-plane shear strength (S_{LT}), shear modulus (E_{LT}), and ultimate shear strain (ϵ_{LT}) when the temperature is raised from 23C to 93C (ref. 3)	24
9	Short beam shear strength retained (percent) after immersion in different fluids for 30 and 180 days (ref. 4)	25
10	Short beam shear modulus retained (percent) after immersion in different fluids for 30 and 180 days (ref. 4)	26
11	Room temperature flexural strength (S_f) and flexural modulus (E_f) (L - longitudinal, T - transverse direction) (ref. 3).	27
12	Fatigue stress for survival to one million cycles (L - longitudinal, T - transverse direction) (refs. 2, 3).	28
13	Baseline ("as received") lap shear strengths of adhesive bonded single lap joints	29

LIST OF TABLES (Concluded)

<u>TABLE</u>		<u>PAGE</u>
14	Changes in lap shear strength (S/S_B) and modulus (E/E_B) of adhesive bonded single lap joints after 30 days of environmental exposure at 23C (B - Baseline value) (ref. 11)	30
15	Loss factor and storage modulus at 23C, and maximum changes in these parameters when the temperature is increased from 23C to 120C (L - longitudinal T - transverse direction) (refs. 3, 13)	31
16	Maximum changes in dynamic properties during 1000 hours of soak (L - longitudinal, T - transverse direction) (ref. 12)	32
17	Impact properties of SMC composites. Temperature 23C impact velocity 1 m/s (ref. 3)	33
18	Thermal expansion coefficient α at room temperature (L - longitudinal, T - transverse direction) (refs. 2, 3)	34

I. INTRODUCTION

Owing to their favorable performance characteristics, light weight composite materials have been gaining wide applications in commercial, space, and military applications. For example, the use of fiber reinforced plastics (FRP), in automobiles increase considerably during the past decade. To date, FRP materials have been used mostly in applications where the material is not subjected to heavy loads. In order to take full advantage of FRP materials, they should be used also as load bearing members. Such applications require a comprehensive data base. For this reason, in recent years several investigators have measured the properties of glass fiber reinforced sheet molding compounds (SMC). In this report a summary is given of the engineering properties of SMC materials and of the effects of service environment on these properties. Continuous fiber composites (e.g. graphite-epoxy composites) are not included in this survey.

In presenting the results emphasis is placed on the main features and characteristics of the data. Readers interested in details of the material behavior are referred to the appropriate references quoted in the text, figure captions, and table headings.

II. MATERIALS AND PROCESSING

Sheet molding compounds consist of polyester (or, less frequently vinyl-ester or epoxy) resins reinforced with glass fibers. A given material may contain randomly oriented chopped fibers (designated as SMC-R), continuous fibers (SMC-C and XMC) or a combination of chopped and continuous fibers (SMC-C/R and XMC-3), as illustrated in Fig. 2. Numbers added after the letters R and C indicate the weight percent of chopped and continuous fibers, respectively. XMC contains 75% glass fibers by weight. The continuous fibers provide added strength and stiffness in the direction of maximum load. The random fibers provide strength and stiffness in the direction perpendicular to the fibers. The formulations and densities of different types of materials are given in Tables 1 and 2.

SMC materials are processed on machines illustrated in Figs. 3-5. The materials are compounded on machines shown in Fig. 3 (used for all types of SMC materials except XMC-3) and in Fig. 4 (used for XMC-3). The compounded material is allowed to set at room temperature for five to ten days. The required part is then manufactured by compression molding in metal dies (Fig. 5). The die temperature may range from 130 to 165°C and the die pressure from 3 to 14 MPa. The process time may vary from one to three minutes. The exact conditions depend upon the material, the thickness, and the shape of the part.

The material formulation as well as the control of the compounding and molding processes affect significantly the properties of the finished product. Care must be exercised, therefore, during the manufacturing process to avoid undesirable and unacceptable variations in material properties.

III. STATIC PROPERTIES

In this section the tensile, compression, shear and flexural properties of SMC materials are reviewed.

1. Tensile Strength and Modulus

The room temperature tensile strength, tensile modulus, tensile strain at failure, and Poisson's ratio are summarized in Table 3. Materials which contain continuous fibers (XMC-3 and SMC-C20/R30) have different properties in the directions along and perpendicular to the fibers (Fig. 6). Therefore, properties for these materials are listed separately for the longitudinal and transverse directions. For materials containing both continuous and chopped fibers, the amount of chopped fibers also affects the tensile properties, as shown in Fig. 7.

Both the ultimate tensile strength and the tensile modulus depend on the material formulation. In addition, the environment has a marked effect on these properties. Generally, both the ultimate tensile strength and the tensile modulus decrease at elevated temperatures (Fig. 8) and during exposure to fluids commonly encountered in automotive applications (Tables 4,5). The decrease in properties depends on the temperature, the type of fluid, and the length of exposure. Interestingly, under some conditions there is a slight (~10%) increase in both the tensile strength and the tensile modulus. The increase is probably due to plasticization of the material.

2. Compression Strength and Modulus

The room temperature compression strength, compression modulus, and the strain at failure of different types of materials are listed in Table 6. Both the strength and the modulus depend on the material composition, on the fiber orientation, and

on the temperature (Fig. 9). As expected, the strength and the modulus are highest along the fiber direction of composites containing continuous fibers (XMC-3 and SMC-C20/R30).

3. Shear Strength and Shear Modulus

Room temperature values of in-plane shear strength, in-plane shear modulus, short beam shear strength, and short beam shear modulus are given in Table 7. In most cases there is a significant decrease in strength and in modulus at elevated temperature (Table 8) and during exposure to humid air and to different types of liquids (Tables 9,10). As in the case of tensile properties, shear properties also increase slightly under some conditions. Again, this increase is caused by plasticization of the material.

4. Flexural Strength and Modulus

The flexural strengths and flexural moduli of different types of SMC materials are presented in Table 11. These properties are highest in the longitudinal directions of XMC-3 and SMC-C2/R30 composites, and are about five times higher in the longitudinal than in the transverse direction. The strength and the modulus decrease with increasing temperature (Fig. 10). For XMC-3 composites the strength and the modulus also depend on the weight percent of chopped fibers (Fig. 11).

5. Notch Sensitivity

The notch sensitivities of three types of SMC materials were investigated by Riegner and Sanders [3]. The reduction in tensile strength (due to circular holes or "notches") of XMC-3, SMC-C20/R30 and SMC-R65 materials are shown in Fig. 12. The solid lines in this figure represent results obtained by matching the three parameter model of Pipes et. al. [3,6] to the data.

Riegner and Sanders also measured the notch strength of SMC-R25 materials. This material did not fail through the circular holes. Apparently, the weakening effects of the holes were less than the strength of the material itself.

IV. FATIGUE

Most of the data available on the fatigue behavior of SMC materials are for tests performed in tension-tension mode. A typical test record is shown in Fig. 13. In this figure the measured loads and deformations have been converted to stresses and strains, respectively.

Fatigue life (S-N) data for tension-tension fatigue are presented in Figs. 14-16. In general, the fatigue strengths follow the same trends as the static strengths. The material that has the highest static strength has also the highest fatigue strength. A good indicator of the relative fatigue performance of different types of materials is the maximum stress the materials can sustain without failure for one million cycles. These data are presented in Table 12. As can be seen, the maximum stress depends not only on the material but also on the temperature.

The effect of temperature on fatigue life is further illustrated in Figs. 15 and 16. For chopped fiber composites (SMC-R25 and SMC-R65) an increase in temperature from 23C to 93C results in about a twofold decrease in the fatigue strength of the material (Fig. 16). The fatigue strengths of materials containing continuous fibers (XMC-3 and SMC-C20/R30) seem to be affected less by changes in temperature (Fig. 15) than by the orientation of the fibers (Fig. 16).

A limited amount of data is available for compression-tension fatigue (Fig. 17). Data generated with SMC-R25 composites indicate that most of the damage is done during the tension portion of the cycle [2]. The compression portion of the

cycle seems to contribute less to the damage.

Results for flexural fatigue are presented in Fig. 18. For SMC-R25, SMC-R57, and SMC-R65 composites at one million cycles the stress levels are about 0.4, 0.35, and 0.25 times the static flexural stress [2]. These values are about twice those reported by Maaghul and Potkanowicz [10] for SMC-R25 and SMC-R65 composites.

Room temperature creep during fatigue tests is shown in Fig. 19. As expected the creep increases with increasing load. Furthermore, for SMC-C20/R50 composites the amount of creep is about twice as large in the direction of the fibers than in the transverse direction.

In those applications where stiffness of a part is an important factor changes in modulus during fatigue must be taken into consideration. Sheet molding compounds may decrease in modulus during fatigue cycling (Figs. 20,21). At room temperature the modulus decay is small (less than ~20%) except in the transverse direction of SMC-C20/R30 composites. Hence, in most automotive applications the decay in modulus would not play an important role.

Heimbuch and Sanders [2] evaluated the effects of test frequency on fatigue behavior. For SMC-R25 and SMC-R57 composites test frequencies from 5 to 20 Hz did not change markedly the fatigue life.

Heimbuch and Sanders [2] also examined the effects of notches on the fatigue characteristics of SMC-R25 and SMC-R65 composites by drilling 0.6 mm diameter holes into the samples. These holes did not have a pronounced effect on the fatigue behavior, suggesting that these materials are not notch sensitive in fatigue.

V. CREEP

The results of static creep tests are presented in Figs. 22-28. The curves are average values. There is considerable scatter in the actual data. An arrow at the end of a curve indicates that the specimen did not fail at the end of the test, while a cross indicates specimen failure.

As expected, the strain increases with load, temperature, relative humidity, and time. The increase in strain with time is not uniform. Step "jumps" occur in strain at random times. Because of these unpredictable jumps, the strain cannot be described by simple viscoelastic models.

Heimbuch and Sanders [2] also investigated the stress rupture of SMC-R25, SMC-R57 and SMC-R65 composites in air at 23, 60, and 90C and at 50% and 100% relative humidities. Owing to the large scatter in the data, the effect of the environment on stress rupture cannot be ascertained from the results of these tests.

VI. ADHESIVE BONDED SINGLE LAP JOINTS

In this section, the behavior of adhesive bonded single lap joints exposed to automotive related fluids is discussed. The results presented were obtained with adherends bonded with a two part urethane adhesive, characterized in detail in ref. [11].

1) Moisture Absorption Characteristics

Typical moisture absorption data obtained with XMC-3 to SMC-R50 joints are given in Fig. 29. Data for SMC-R50 to SMC-R50 joints exhibit similar trends.

At 23C both XMC-3 to SMC-R50 and SMC-R50 to SMC-R50 joints seem to approach asymptotically the same maximum moisture content (M_m) when immersed in the same fluid. During a two month test period M_m is reached only in air. In water and in 5% NaCl-water mixture the maximum moisture contents are not attained. The M_m values can be estimated by extrapolating the data, giving 0.18, 1.5 and 2.0 percent for air, salt water, and water, respectively.

A 93C (immersion in water) the maximum moisture level is not approached asymptotically. Here the weight increases for about the first 100 hours and then decreases at a rapid rate. This indicates that the material deteriorates during exposure. At 93C both bonded and unbonded test specimens behave similarly, suggesting that degradation is mostly in the composite and not in the adhesive.

Joints loaded up to 30 percent of their strength did not show appreciable change in their moisture absorption characteristics.

2) Lap Shear Strength

Lap shear strengths of adhesive bonded single lap joints are given in Table 13. Changes in baseline strength and modulus during environmental exposure are illustrated in Table 14. Neither the strengths nor the moduli change significantly when the joints are exposed to room temperature fluids. In some cases the strength improves slightly (10-15%) during environmental conditioning. The beneficial effects of fluid and temperature are likely due to plasticization. The strength of joints immersed in hot (93C) water and salt water for 30 days decrease by a factor of two. Loading (up to 30 percent of the baseline strength) during exposure does not seem to affect the strength.

The joints may fail by delamination of the composite or by separation of

the adherent. In these tests, most failures occurred by delamination of the adherent. Separation of the adhesive was predominant only at higher (93C) temperatures.

3) Fatigue

Wang et al [11] conducted fatigue life tests on SMC-R25 to SMC-R25 and SMC-R50 to SMC-R50 single lap joints. During the tests the stress levels were 30, 50, 70 and 90 percent of the static shear strength. Prior to the fatigue tests the specimens were soaked for 30 days at room temperature in the following liquids: 50% by weight salt water, motor oil, transmission fluid, and gasoline. The ranges of data are shown in Fig. 30. The data are not shown separately for specimens immersed in the different fluids because the fluids did not have a significant effect on the fatigue life.

The residual strengths and moduli were also measured for those specimens surviving for one million cycles [11]. Cyclic stressing at 30 percent of ultimate strength does not degrade appreciably either the strength or the modulus; in general, both the strength and the modulus retained at least 80 percent of their initial values.

4) Creep

Creep deformations of adhesive bonded single lap joints under static and cyclic loadings are shown in Figs. 31 and 32. These figures illustrate the effects of material, fluid, temperature, and applied load on creep behavior. The type of material used in forming the joints has smaller effect on creep than does the type of fluid, the temperature, and the applied load. The creep is lowest in air, and is higher in water, in salt water, and in hydrocarbons.

The creep also increases with temperature and with applied load. For example, at 23C none of the XMC-3 to SMC-R50 or SMC-R50 to SMC-R50 joints failed during static creep. In air at 93C only one of the joints failed, this occurring at 30 percent load level. During water immersion (at 93C) all but 3 coupons failed before the end of the 715 hours test. During cyclic creep, only joints with 30 percent load survived for one million cycles. At higher loads none of the joints survived for one million cycles (Fig. 32).

VII. VIBRATION DAMPING

Materials used in commercial applications should damp out noise and vibrations. It is important, therefore, to know the vibration damping properties of SMC materials. These properties may be characterized by two parameters, the loss factor and the storage modulus. These parameters are obtained by exciting the material with forced sinusoidal oscillations and by measuring the input stress and output strain [3]. The loss factor is the tangent of the phase angle between the stress and the strain, and is equal to the ratio between the energy dissipated and the energy stored in the material. The storage modulus is the in-phase component of the ratio of input stress to output strain.

Room temperature values of loss factors and storage moduli are listed in Table 16. The loss factor is insensitive to the exciting frequency in the range of 0.1 to 10 Hz. For the SMC materials tested the loss factors are an order of magnitude higher than for steel. Thus, SMC materials would damp out vibrations more effectively than steel.

The effects of temperature and soaking in different types of liquids are illustrated in Tables 15 and 16. An increase in temperature (from 23C to 120C)

increases the damping and reduces the stiffness. Soaking in liquids has similar effects. Soaking for 1000 hours considerably increased the damping of chopped fiber composites (SMC-R25 and SMC-R60), while their stiffness decreased slightly. The damping characteristics of continuous fiber composites (XMC-3 and SMC-C20/R30) change little in the fiber direction. It is noteworthy that both temperature and moisture-induced changes in the vibration properties appear to be reversible [12].

VIII. DYNAMIC IMPACT

Fiber reinforced composites used in automotive applications should be able to resist impact damage. Unfortunately, glass fiber reinforced polyester composites absorb less energy during impact than metals. This is illustrated in Fig. 33, where a comparison is made between the energies absorbed by different types of materials during impact against a fixed barrier. At a given deformation, metals absorb about twice as much energy as the composite.

Impact resistances of composites may be evaluated using the Rheometrics High Rate Impact Tester [3,5]. In tests with this device a hydraulic ram impacts a clamped plate of material and the load versus displacement is recorded, as shown in Fig. 34. From the data several parameters can be calculated, including yield and ultimate load, apparent impact modulus, yield and ultimate displacement, yield and ultimate energy absorbed. Typical values of some of these parameters are given in Table 17. The data in this table are a summary of the results of Riegner and Sanders [3], who reported data for different impact velocities (from 0.5 to 10 m/s) and for different temperatures (23 and -35C). The data do not show clear trends. In general, neither changes in impact velocity nor changes in temperature had a significant effect on the load, modulus, displacement, and energy

values given in Table 17.

IX. MOISTURE ABSORPTION

Glass fiber reinforced organic matrix composites absorb moisture when exposed to humid air or to liquids. The weight changes of different types of SMC composites exposed to typical automotive service environments are presented in Figs. 35-37. The weight change (M) is defined as

$$M = \frac{\text{wet weight} - \text{dry weight}}{\text{dry weight}} \times 100 \text{ percent}$$

The data show that, in general, when the dry material is submerged in the fluid the weight at first increases then levels off for some length of time. Both the initial rate of weight increase and the value at which the weights level off depend on a) the material, b) the temperature, and c) the environment (relative humidity of air or the type of liquid used). The data also show that in some instances the weight does not remain constant after it reaches a level value but keeps either increasing or decreasing. This suggests that under some conditions the moisture transport is by a non-Fickian process. One reason for the non-Fickian behavior may be that moisture transfer through the resin does not proceed by a process that can be described by Fick's law. Another plausible explanation of the observed non-Fickian absorption process is as follows. Owing to the moist, high temperature environment, microcracks develop on the surface and inside the material. Moisture rapidly enters the material, causing an increase in weight. As the cracks grow larger, material, most likely in the form of resin particles, is actually lost. In fact, such material loss is frequently observed after a few hours of exposure to the moist environment. As long as the moisture

gain is greater than the material loss, the weight of the specimen increases. Once the weight of the lost material exceeds the weight of the absorbed moisture, the weight of the specimen decreases. Of course, when the material is lost, the measured weight change no longer corresponds to the moisture content of the material.

The foregoing results were all obtained with unstressed specimens. However, as was indicated in Section VI.1, the moisture absorption characteristics of stressed and unstressed SMC materials do not differ appreciably.

X. THERMAL EXPANSION

The dimensional changes of the material during temperature cycles must be taken into account in the design process. The thermal expansion coefficient values reported by Heimbuch and Sanders [2] and by Riegner and Sanders [3] are reproduced in Table 18. As expected, the thermal expansion coefficients are lowest along the fiber direction of composites containing continuous fibers (XMC-3 and SMC-C20/R30). The coefficient is high in the transverse direction of these materials and also for SMC-R25 composites. More comprehensive data on the variation of the thermal expansion coefficient with temperature are not yet available.

XI. CONCLUDING REMARKS

As this survey indicates, the numerous studies made in recent years provide much of the needed information on the mechanical and thermal properties of glass fiber reinforced SMC composites. For many materials we now have the extensive data bases required for the design of practical engineering systems. There are still areas in need of further exploration. In particular, information is needed on problems in which the viscoelastic behavior of the material predominates. Hopefully, the continuing efforts in this area will soon provide information which will lead to an understanding of these problems.

REFERENCES

1. Charlesworth, D., "Review of Plastics Applications Within BL Cars", in Worldwide Applications of Plastics, Society of Automotive Engineers, SP-482 (February 1981) 73-85.
2. Heimbuch, R.A. and Sanders, B.A., "Mechanical Properties of Chopped Fiber Reinforced Plastics", in Composite Materials in the Automotive Industry, American Society of Mechanical Engineers, (December 1978) 111-139.
3. Riegner, D.A. and Sanders, B.A., "A Characterization Study of Automotive Continuous and Random Glass Fiber Composites", Report GMMD79-023, General Motors Corporation, Manufacturing Development, GM Technical Center, Warren, Michigan, 42090 (1979).
4. Springer, G.S., Sanders, J.A. and Tung, R.W. "Environmental Effects of Glass Fiber Reinforced Polyester and Vinylester Composites", J. Composite Materials, 14 (July 1980) 213-232.
5. Denton, D.L., "Mechanical Properties Characterization of an SMC-R50 Composite", 34th Annual Technical Conference, Reinforced Plastics/Composites Institute, The Society of the Plastics Industry, 1979, Section 11-F; also SAE Paper 790671 (1979).
6. Enos, J.H., Erratt, R.L., Francis, E. and Thomas, R.E., "Structural Performance of Vinylester Resin Compression Molded High Strength Composites", 34th Annual Technical Conference, Reinforced Plastics/Composites Institute, The Society of Plastics Industry, 1979, Section 11-E.
7. Ackley, R.H. and Carley, E.P., "XMC-3 Composite Material Structural Molding Compound", 34th Annual Technical Conference, Reinforced Plastics/ Composites Institute, The Society of Plastics Industry, 1979, Section 21-D.

8. Adams, D.F. and Walrath, D.E., "Iosipescu Shear Properties of SMC Composite Materials", Department of Mechanical Engineering, The University of Wyoming, Larrabee, Wyoming 82738 (1981).
9. Pipes, R.B., Wetherhold, R.C. and Gillespie, J.W., "Notched Strength of Composite Materials", J. Composite Materials, 13 (April 1979) 148-160.
10. Maaghul, J. and Potkanowicz, E.J., "HMC - A High Performance Sheet Molding Compound", 31st Annual Technical Conference, Reinforced Plastics/Composites Institute, The Society of Plastics Industry, 1976, Section 7-C.
11. Wang, T.K., Sanders, B.A. and Lindholm, U.S., A Loading Rate and Environmental Effects Study of Adhesive Bonded SMC Joints, Report GMMD80-044, General Motors Corporation, Manufacturing Development, GM Technical Center, Warren, Michigan, 48090 (1980).
12. Gibson, R.F., Yau, A. and Riegner, D.A., "The Influence of Environmental Conditions on the Vibration Characteristics of Chopped-Fiber-Reinforced Composite Materials", Presented at AIAA/ASME/ASCE/AHS 22nd Structures, Structured Dynamics and Materials Conference (April 1981).
13. Seiffert, V.W., "Review of Recent Activities and Trends in the Field of Automobile Materials", in Worldwide Applications of Plastics, Society of Automotive Engineers, SP-482 (February 1981) 1-6.
14. Loos, A.C., Springer, G.S., Sanders, B.A. and Tung, R.W., "Moisture Absorption of Polyester-E Glass Composites", J. Composite Materials, 14 (April 1980) 142-154.

Table 1. Material formulations and densities of SMC materials.

(PPG-PPG Industries, OFC-Owens Corning Fiberglas) (refs. 2,3)

Material	Ingredient	Type	Weight %	Density kg/m ³
XMC-3	Continuous Glass Fibers- +7.5°, X-Pattern	PPG XMC Strand Type 1064	50	1970
	2.54 cm Chopped Glass Fibers	PPG XMC Strand Type 1064	25	
	Resin	PPG Selectron RS-50335 Isophthalic Polyester	21.5	
	Monomer	Styrene	2.4	
	Thickener	PPG Selectron RS-5988	0.8	
	Catalyst	TRPB	0.2	
	Mold Release	Zinc Stearate	0.1	
SMC-C20/R30	Continuous Glass Fibers - Aligned	OCF 433AB Roving	20	1810
	2.54 cm Chopped Glass Fibers	OCF 433AB Roving	30	
	Resin	OCF-E980 Polyester	32.3	
	Filler	Calcium Carbonate	16.1	
	Mold Release	Zinc Stearate	0.8	
	Thickener	Magnesium Oxide	0.5	
	Catalyst	TBP	0.3	
	Inhibitor	Benzoquinone	Trace	
SMC-R25	2.54 cm Chopped Glass Fibers	E-Glass (OCF 951 AB)	25	1830
	Resin	Polyester (OCF E-920-1)	29.4	
	Filler	Calcium Carbonate	41.8	
	Internal Release	Zinc Stearate	1.1	
	Catalyst	Tertiary Butyl Perbenzoate	0.3	
	Thickener	Magnesium Hydroxide	1.5	
	Pigment	Mapico Black	0.8	
SMC-R50	2.54 cm Chopped Glass Fibers	OCF 433AB	50	1870
	Resin	OCF-E980 Polyester	32.3	
	Filler	Calcium Carbonate	16.1	
	Mold Release	Zinc Stearate	0.8	
	Thickener	Magnesium Oxide	0.5	
	Catalyst	TBP	0.3	
	Inhibitor	Benzoquinone	Trace	
SMC-R57	Formulated Epoxy Resin	Epoxy Sheet Molding Compound (Gulf 1057)	43	1740
	1.27 cm Chopped Glass Fibers	E-Glass (OCF-495)	57	
SMC-R65	2.54 cm Chopped Glass Fibers	E-Glass (PPG 518)	65	1820
	Rigid Resin	Polyester (PPG 50271)	16	
	Flexible Resin	Polyester (PPG 50161)	16	
	Thickener, etc.		3	
EA-SMC-R30	2.54 cm Chopped Glass Fibers	E-Glass (OCF 956)	28	1830
	Resin	Polyester	19.9	
	Filler	Calcium Carbonate	41	
	Thickener	Balance	11.1	

Table 2. VE-SMC-R50 paste formulation

Component	Parts
A-SIDE	
XD-9013.03	10
TBPB	1
Camelwite	92
Zinc Stearate	3
B-SIDE	
Derakane [*] 470-45	100
Maglite D	50
Camelwite	100
Pump 10-14/1 by weight A/B	
Max viscosity = 6000 cps	
(90F, RVT, # 4 Spindle, 20 rpm)	

*Registered Trademark of Dow Chemical Company

Table 3. Room temperature ultimate tensile strength (S_t), tensile modulus (E_t), tensile failure strain (ϵ_t), and Poisson's ratio (ν_t) (L - longitudinal, T - transverse direction) (refs. 2-6)

Material	S_t (MPa)	E_t (GPa)	ϵ_t (%)	ν_t
XMC-3(L)	561	35.7	1.66	0.31
XMC-3(T)	70	12.3	1.54	0.116
SMC-C20/R30(L)	289	21.4	1.73	0.3
SMC-C20/R30(T)	84	12.4	1.58	0.18
SMC-R25	82	13.3	1.34	0.25
SMC-R50	164	15.8	1.73	0.31
SMC-R57	160	16.5	-	-
SMC-R65	227	14.7	1.67	0.26
EA SMC-R30	30	8.7	1.43	0.30
VE-SMC-R50	165	7.0	-	-
VE-SMC-C40/R10(L)	426	-	-	-
VE-SMC-C40/R10(T)	57	-	-	-
VE-XMC-3(L)	648	-	-	-
VE-XMC-3(T)	74	-	-	-

Table 4. Tensile strength retained (percent) after immersion in different fluids for 30 and 180 days. (L - longitudinal, T - transverse direction) (refs. 3, 4)

Fluid	XMC-3 30 days	SMC-C20/R30 30 days	SMC-R25 30 days	SMC-R50 30 days	VE-SMC-R50 30 days
Water, 23C	89 (L) 107 (T)	103 (L) 73 (T)	-	-	-
Humid Air, 23C, 50% r.h	-	-	100	100	105
Humid Air, 93C, 50% r.h	-	-	95	100	102
Humid Air, 23C, 100% r.h	-	-	90	80	75
Humid Air, 93C, 100% r.h	-	-	95	95	95
Salt Water 23C	95 (L) 107 (T)	90 (L) 87 (T)	95	105	102
Salt Water, 93C	-	-	70	105	85
No. 2 Diesel, 23C	-	-	90	98	103
No. 2 Diesel, 93C	-	-	95	98	101
Motor Oil, 23C	95 (L) 110 (T)	100 (L) 108 (T)	95	95	95
Motor Oil 93C	-	-	90	90	105
Antifreeze, 23C	95 (L) 110 (T)	78 (L) 108 (T)	95	95	95
Antifreeze, 93C	-	-	75	85	45
Gasoline, 23C	97 (L) 108 (T)	101 (L) 96 (T)	90	100	100
Gasoline, 93C	-	-	75	95	105
Transmission Fluid, 23C	99 (L) 120 (T)	82 (L) 110 (T)	-	-	-
Break Fluid, 23C	97 (L) 93 (T)	97 (L) 109 (T)	-	-	-

Table 5. Tensile modulus retained (percent) after immersion in different fluids for 30 and 180 days (ref. 4)

Fluid	SMC-R25		SMC-R50		VE-SMC-R50	
	30 days	180 days	30 days	180 days	30 days	180 days
Humid Air, 23C, 50% r.h	105	110	100	90	98	95
Humid Air, 93C, 50% r.h	120	110	90	80	95	90
Humid Air, 23C, 100% r.h	100	95	90	80	95	90
Humid Air, 93C, 100% r.h	120	110	85	80	90	90
Salt Water, 23C	90	95	90	80	95	90
Salt Water, 93C	110	90	85	65	90	85
No. 2 Diesel, 23C	110	115	90	90	95	95
No. 2 Diesel, 93C	120	95	95	90	90	90
Motor Oil, 23C	95	110	80	90	90	95
Motor Oil, 93C	110	115	90	90	95	95
Antifreeze, 23C	90	110	85	80	90	95
Antifreeze, 93C	85	85	80	50	90	75
Gasoline, 23C	95	90	85	85	95	90
Gasoline, 93C	80	80	88	60	85	75

Table 6. Room temperature compression strength (S_c),
compression modulus (E_c) and compression
failure strain (ϵ_c) (L - longitudinal,
T - transverse direction) (refs. 2, 3)

Material	S_c (MPa)	E_c (GPa)	ϵ_c (%)
XMC-3(L)	480	37	1.36
XMC-3(T)	160	14.5	1.38
SMC-C20/R30(L)	306	20.4	2.50
SMC-C20/R30(T)	166	12.2	1.74
SMC-R25	183	11.7	2.16
SMC-R50	225	15.9	-
SMC-R65	241	17.9	1.81

Table 7. Room temperature in plane shear strength (S_{LT}), in plane shear modulus (E_{LT}), short beam shear strength (S_g), and short beam shear modulus (G_g) (refs. 3, 4, 8)

Material	S_{LT} (MPa)	E_{LT} (GPa)	S_g (MPa)	G_g (GPa)
XMC-3	91.2	4.47	55	-
SMC-C20/R30	85.4	4.09	41	-
SMC-R25	79	4.48	30	5.0
SMC-R50	62	5.94	25	7.0
SMC-R65	128	5.38	45	-
VE-SMC-R50	-	-	35	4.0

Table 8. Losses in in-plane shear strength (S_{LT}), shear modulus (E_{LT}), and ultimate shear strain (ϵ_{LT}) when the temperature is raised from 23C to 93C (ref. 3)

	LOSS (Percent)		
	S_{LT}	E_{LT}	ϵ_{LT}
XMC-3	38	48	13
SMC-C20/R30	40	44	0.7
SMC-R50	-	22	-

Table 9. Short beam shear strength retained (percent) after immersion
in different fluids for 30 and 180 days (ref. 4)

Fluid	SMC-R25		SMC-R50		VE-SMC-R50	
	30 days	180 days	30 days	180 days	30 days	180 days
Humid Air 23C, 50% r.h	105	120	110	110	100	103
Humid Air 93C, 50% r.h	120	110	98	110	105	120
Humid Air 23C, 100% r.h	110	110	90	95	95	95
Humid Air 93C, 100% r.h	102	95	92	85	95	95
Salt Water 23C	110	100	95	95	99	98
Salt Water 93C	95	65	80	35	95	75
No. 2 Diesel 23C	115	120	90	75	95	110
No. 2 Diesel 93C	125	125	103	110	100	105
Motor Oil 23C	100	125	85	95	90	115
Motor Oil 93C	110	120	90	110	95	120
Antifreeze 23C	105	110	90	100	95	105
Antifreeze 93C	75		50	15	85	50
Gasoline 23C			80	95	98	99
Gasoline 93C	70	75	85	85	75	75

Table 10. Short beam shear modulus retained (percent) after immersion in different fluids for 30 and 180 days (ref. 4)

Fluid	SMC-R25		SMC-R50		VE-SMC-R50	
	30 days	180 days	30 days	180 days	30 days	180 days
Humid Air 23C, 50% r.h	110	125	105	100	105	115
Humid Air 93C, 50% r.h	125	115	95	95	110	120
Humid Air 23C, 100% r.h	100	115	85	85	90	95
Humid Air 23C, 100% r.h	115	120	95	85	105	105
Salt Water 23C	110	100	85	90	100	95
Salt Water 93C	85	80	65	50	90	95
No. 2 Diesel 23C	125	120	95	95	105	115
No. 2 Diesel 93C	110	115	95	95	110	110
Motor Oil 23C	105	125	75	90	90	110
Motor Oil 93C	105	125	85	95	90	115
Antifreeze 23C	105	115	75	90	90	110
Antifreeze 93C	80	75	54	15	85	55
Gasoline 23C	95	90	80	95	105	110
Gasoline 93C	60	85	70	70	80	75

Table 11. Room temperature flexural strength (S_f) and flexural modulus (E_f) (L - longitudinal, T - transverse direction) (ref. 3)

Material	S_f (MPa)	E_f (GPa)
XMC-3(L)	973	34.1
XMC-3(T)	139	6.8
SMC-C20/R30(L)	645	25.7
SMC-C20/R50(T)	165	5.9
SMC-R25	220	4.8
SMC-R50	314	14.0
SMC-R65	403	5.7

Table 12. Fatigue stress for survival to one million cycles (L - longitudinal, T - transverse direction) (refs. 2, 3)

Material	Percent Static	Ultimate Tensile Stress
	23C	90C
XMC-3(L)	23	18
XMC-3(T)	27	26
SMC-C20/R30(L)	45	44
SMC-C20/R30(T)	52	43
SMC-R25	49	55
SMC-R50	38	41
SMC-R57	42	-
SMC-R65	31	28
EA-SMC-R30	44	-

Table 13. Baseline ("as received") lap shear strengths of
adhesive bonded single lap joints

	Strength (MPa)	
	<u>23C</u>	<u>93C</u>
XMC to SMC-R50	6.55	3.89
SMC-R50 to SMC-R50	6.11	2.12
SMC-R25 to SMC-R25	3.83	-

Table 14. Changes in lap shear strength (S/S_B) and modulus (E/E_B) of adhesive bonded single lap joints after 30 days of environmental exposure at 23C (B - baseline value) (ref. 11)

Fluid	SMC-R25 to SMC-R25		SMC-R50 to SMC-R50	
	S/S_B	E/E_B	S/S_B	E/E_B
Air	1.00	1.00	1.00	1.00
Motor Oil	0.89	1.05	0.85	0.92
Transmission Fluid	0.92	1.01	0.91	0.91
Gasoline	0.95	0.80	1.20	0.77
Salt Water	0.97	0.72	0.98	0.78
Brake Fluid	0.95	0.87	0.96	0.85
Antifreeze	0.96	1.15	0.81	0.81

Table 15. Loss factor and storage modulus at 23C, and maximum changes in these parameters when the temperature is increased from 23C to 120C (L - longitudinal, T - transverse direction) (refs. 3, 13)

Material	Loss Factor at 23C		Storage Modulus at 23C (GPa)	Max. Change		Percent Storage Modulus
	0.1 Hz	10 Hz		Loss Factor	Storage Modulus	
XMC-3(L)	0.028	0.025	36	+129		-7
XMC-3(T)	0.063	0.053	-	+355		-54
SMC-C20/R30(L)	0.034	0.029	-	+ 80		-5
SMC-C20/R30(T)	0.051	0.049	-	+204		-44
SMC-R25	0.037	0.035	4	+471		-48
SMC-R65	0.039	0.034	8	+241		-30
Steel	~0.001					

Table 16. Maximum changes in dynamic properties
during 1000 hours of soak (L - longitudinal,
T - transverse direction) (ref. 12)

Fluid	Material	Maximum Change (percent)	
		Loss Factor	Storage Modulus
Distilled Water 22C	XMC-3(L)	+ 53	0
	SMC-C20/R30(L)	+ 38	0
	SMC-R25	+193	-20
	SMC-R65	+180	- 7
Distilled Water 50C	XMC-3(L)	+ 88	0
	SMC-C20/R30(L)	+112	0
	SMC-R25	+210	-10
	SMC-R65	+247	-12
Salt Water 23C	XMC-3(L)	+ 55	0
	SMC-C20/R30(L)	+ 50	0
	SMC-R25	+117	- 4
	SMC-R65	+178	- 7
Motor Oil 23C	XMC-3(L)	0	0
	SMC-C20/R30(L)	0	0
	SMC-R25	+ 25	0
	SMC-R65	+ 24	0
Antifreeze	XMC-3(L)	0	0
	SMC-C20/R30(L)	0	0
	SMC-R25	+ 29	0
	SMC-R65	+ 22	0
Gasoline 22C	XMC-3(L)	0	0
	SMC-C20/R30(L)	0	0
	SMC-R25	178	-15
	SMC-R65	30	0

Table 17. Impact properties of SMC composites. Temperature 23C impact velocity 1 m/s (ref. 3)

Material	Load (N)		Apparent Modulus (N/m)		Displacement (mm)		Energy (J)	
	Yield	Ultimate	Yield	Ultimate	Yield	Ultimate	Yield	Ultimate
XMC-3	1.5×10^3	7×10^3		1.2×10^6	1.5	9.0	1	30
SMC-C20/R30	1.2×10^3	5×10^3		1×10^6	1.5	9.0	1	30
SMC-R25	1.2×10^3	5×10^3		1×10^6	1.5	9.0	1	30

Table 18. Thermal expansion coefficient α at room temperature
(L - longitudinal, T - transverse direction) (refs. 2, 3)

Material	α ($\mu\text{m}/\text{m}^\circ\text{C}$)
XMC-3(L)	8.7
XMC-3(T)	28.6
SMC-C20/R30(L)	11.3
SMC-C20/R30(T)	24.6
SMC-R25	23.2
SMC-R50	14.8
SMC-R65	13.7

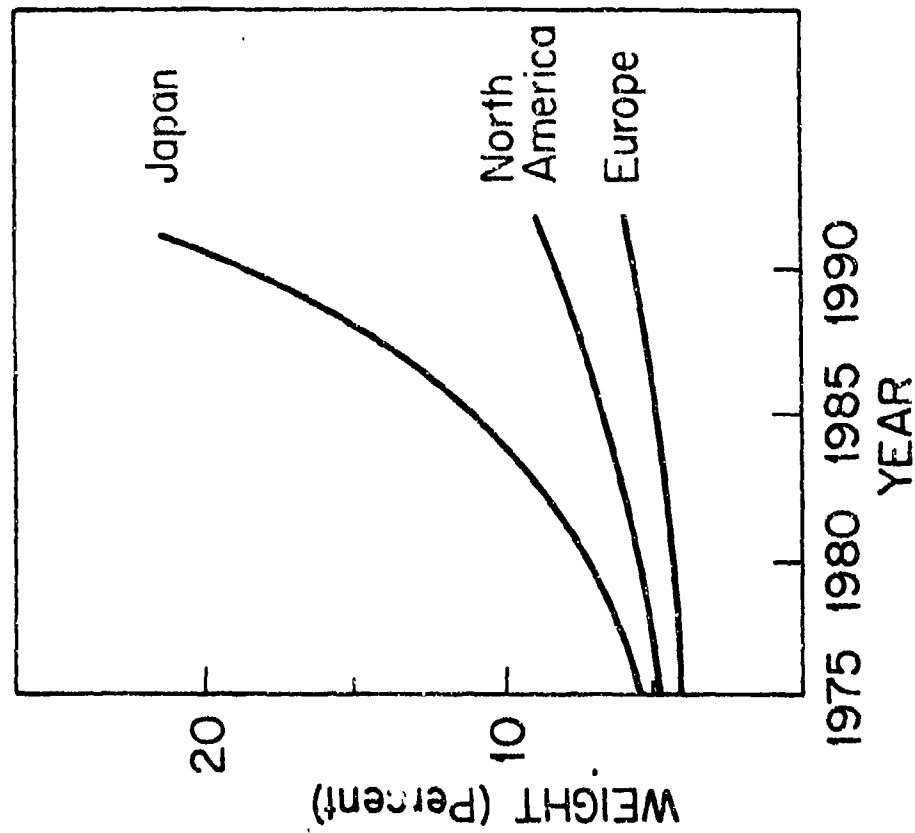
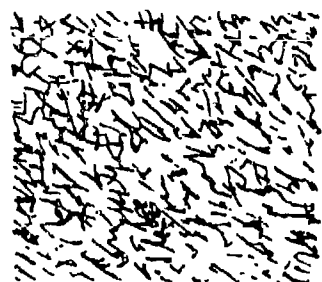
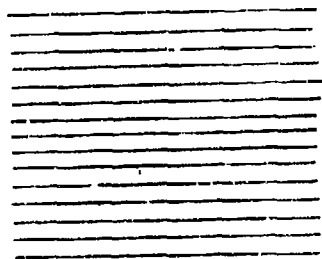


Figure 1: The use of plastics in passenger cars (ref. 1)

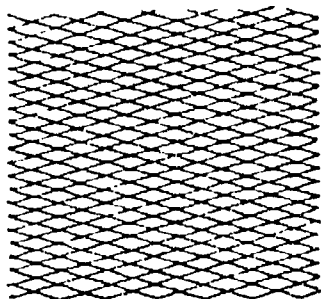
ONE FIBER TYPE



SMC-R

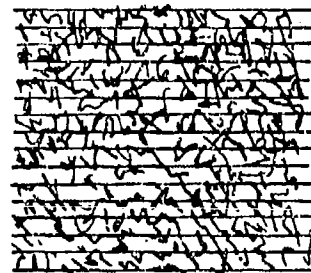


SMC-C

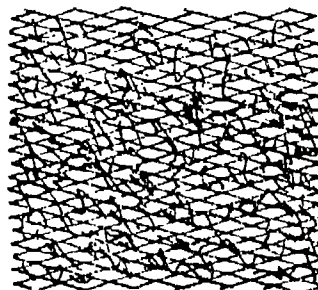


XMC

CONTINUOUS AND RANDOM FIBERS



SMC-C/R



XMC-3

Figure 2: Illustration of glass fiber reinforced sheet molding compounds

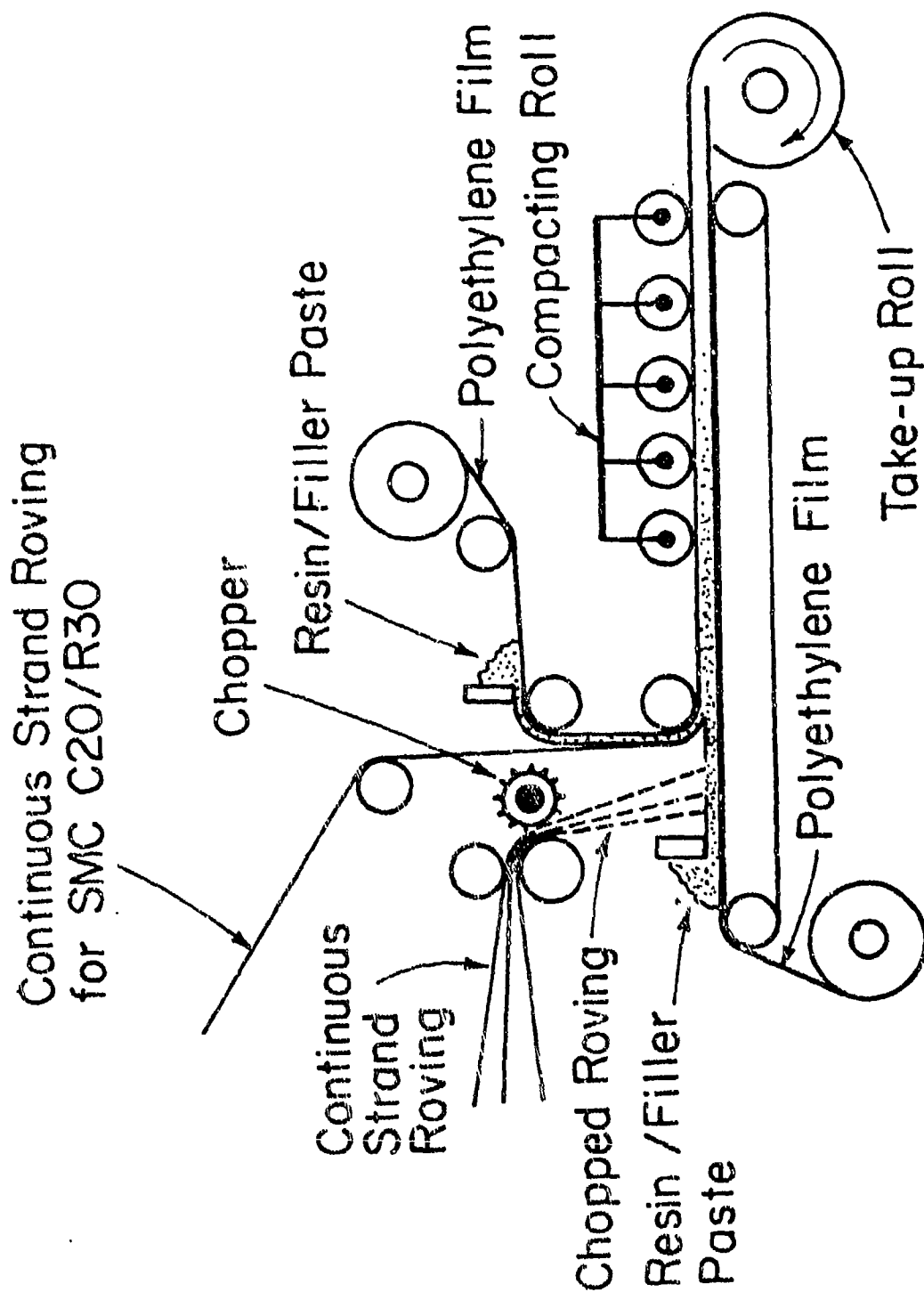


Figure 3: Schematic of process used to manufacture glass fiber reinforced SMC composites (Owens Corning Fiberglass System)

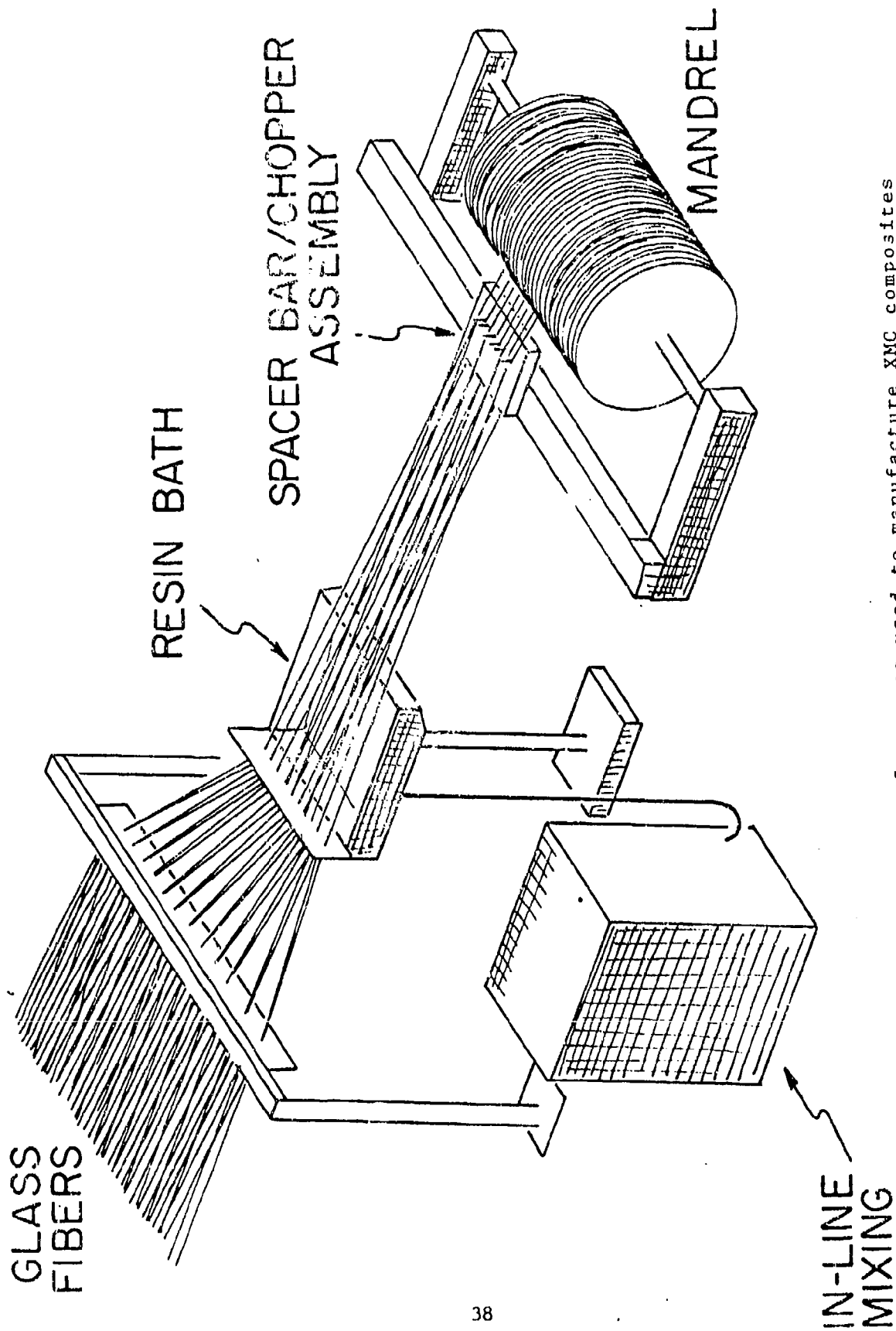


Figure 4: Schematic of process used to manufacture XMC composites
(PPG Industries System)

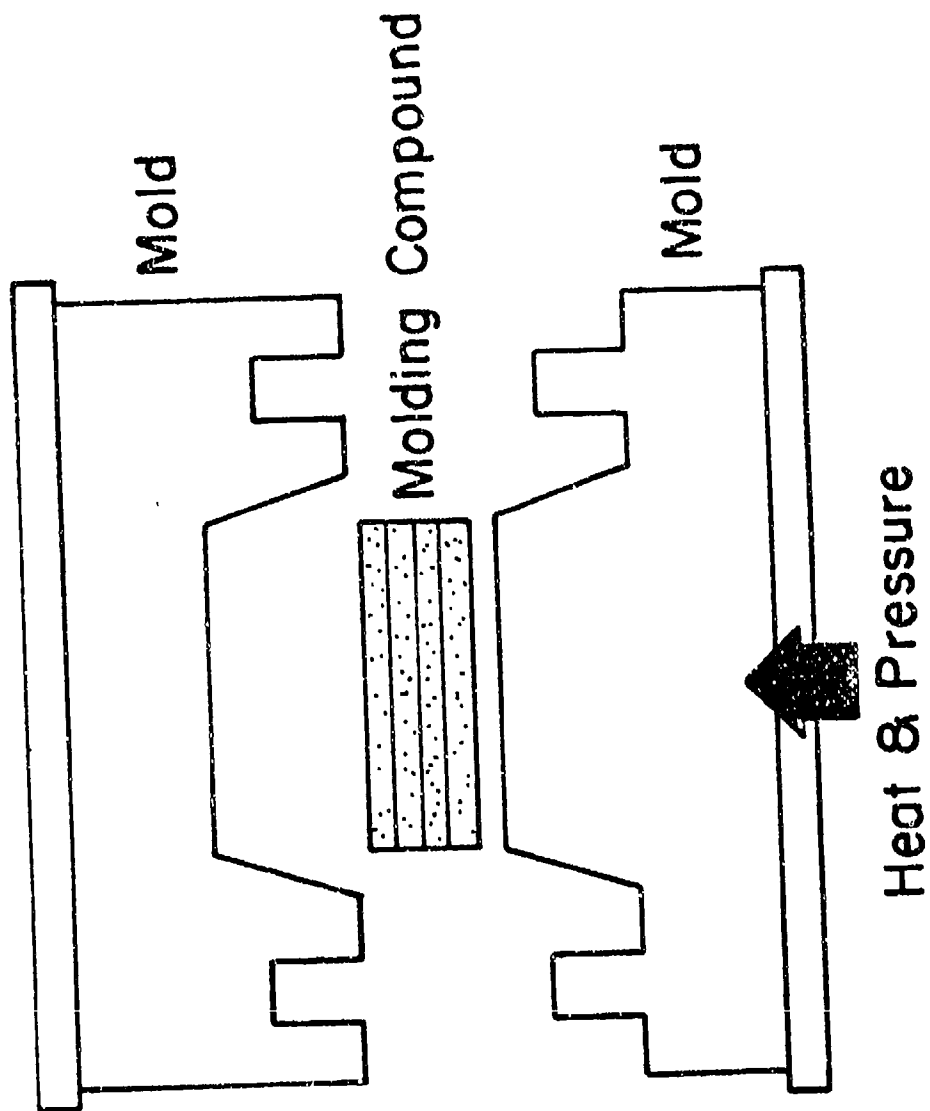


Figure 5: Schematic of compression molding of SMC composites

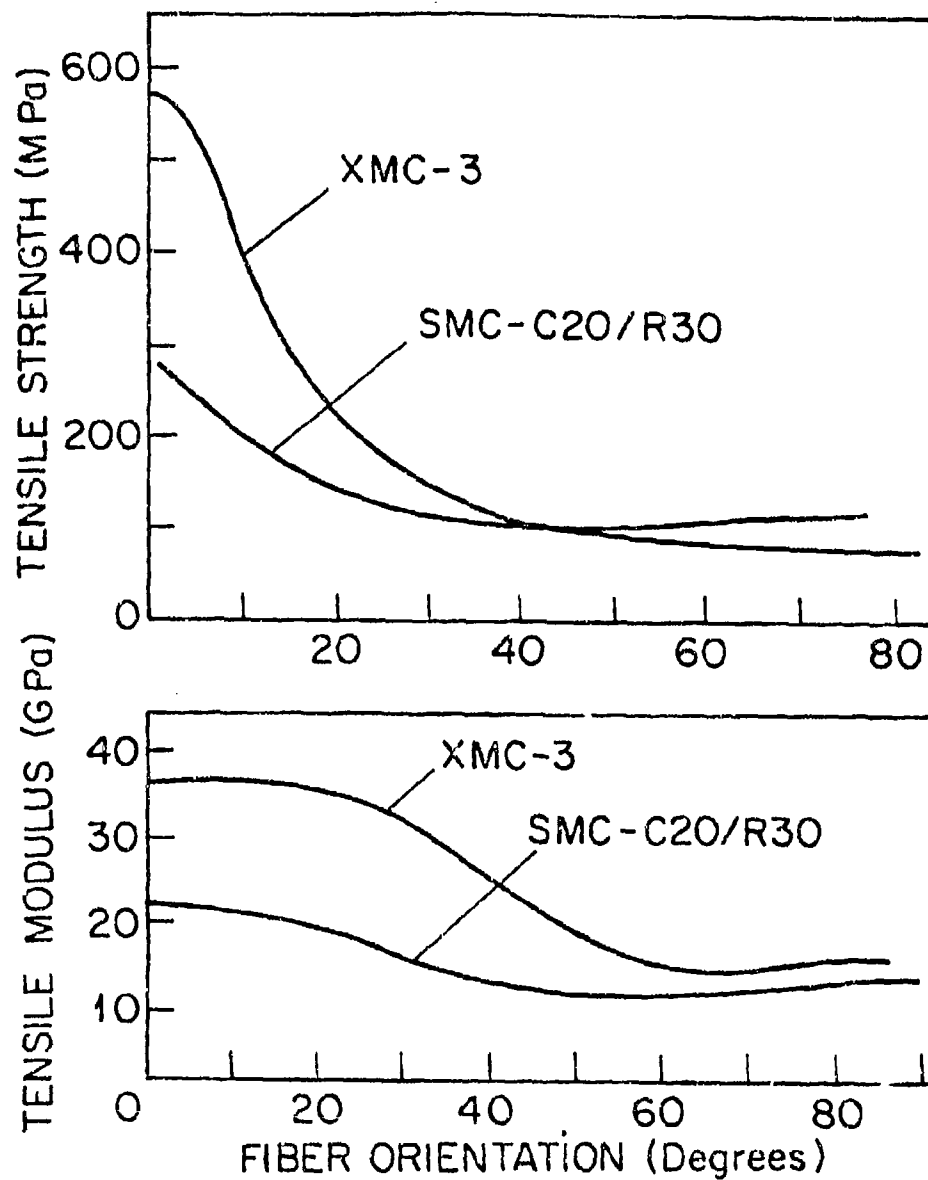


Figure 6: The effect of fiber orientation on the tensile strength and tensile modulus of XMC-3 and SMC-C20/R30 composites (ref. 3)

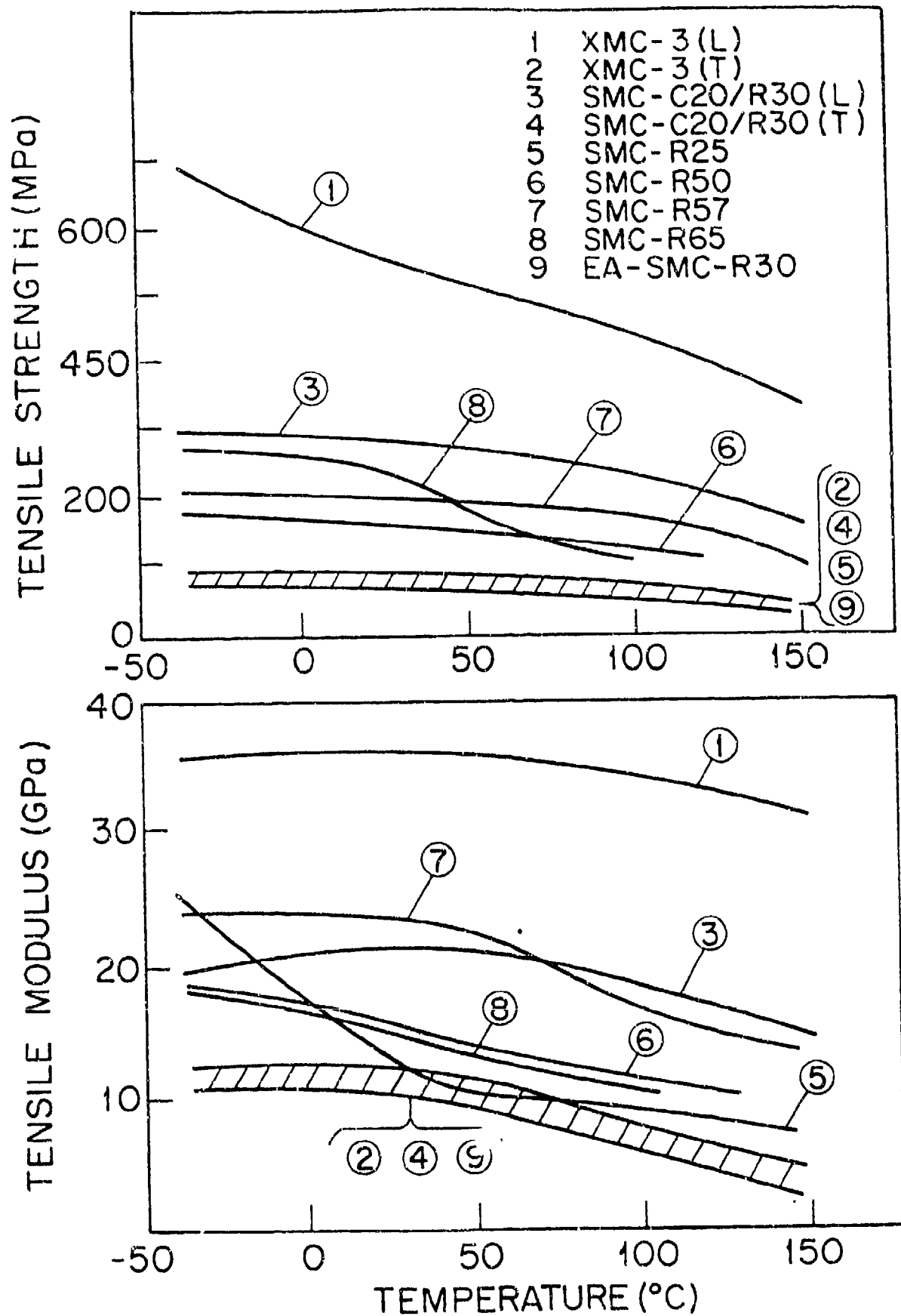


Figure 7: The effect of the amount of chopped fibers on the tensile strength of XMC-3 composites. Total fiber content by weight = 75 percent (ref. 7)

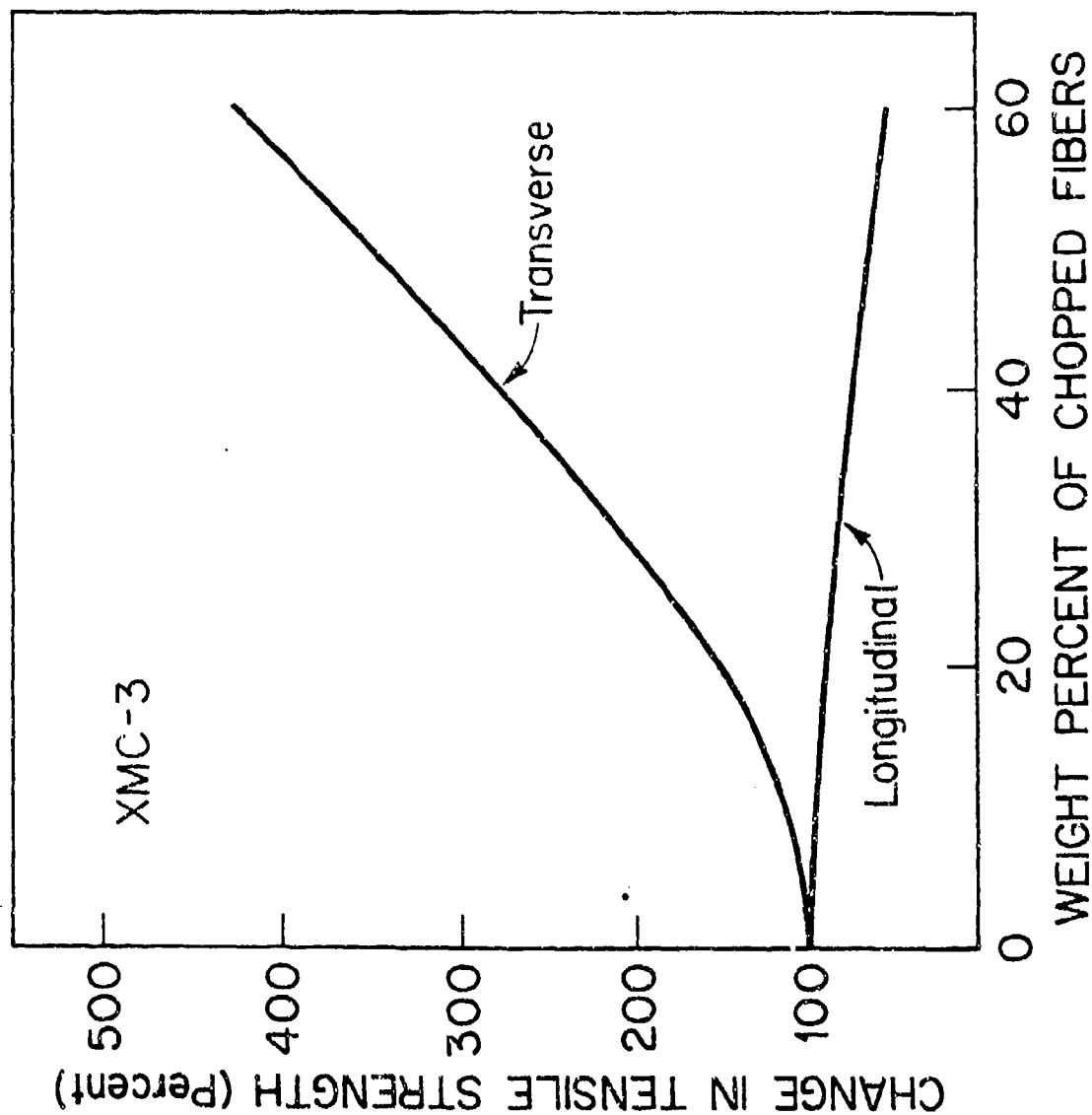


Figure 8: The effect of temperature on the tensile strength and tensile modulus. (L-longitudinal, T- transverse direction) (refs, 2, 3, 5)

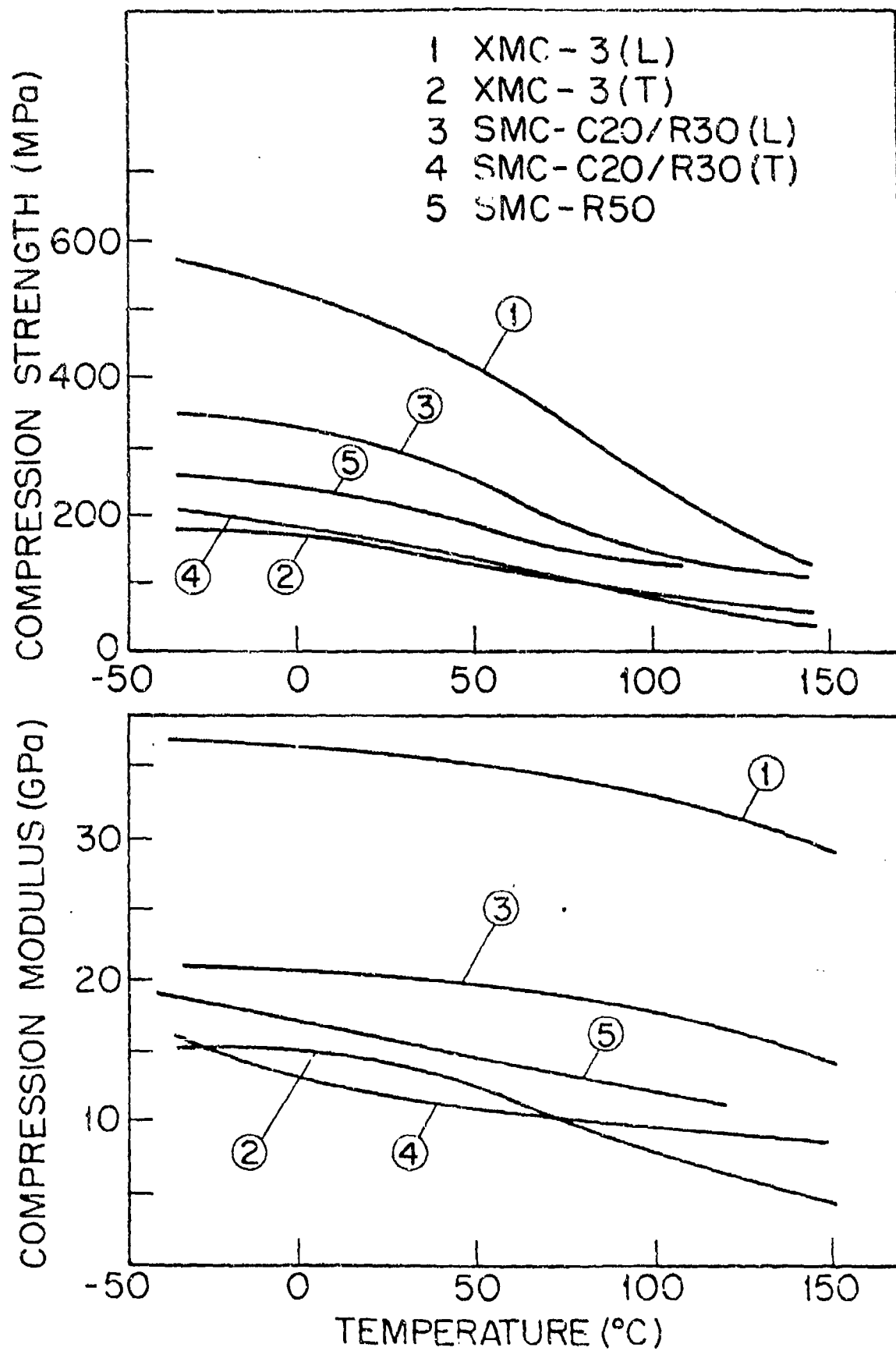


Figure 9: The effect of temperature on the compression strength and compression modulus. (L- longitudinal, T-transverse direction) (ref. 3)

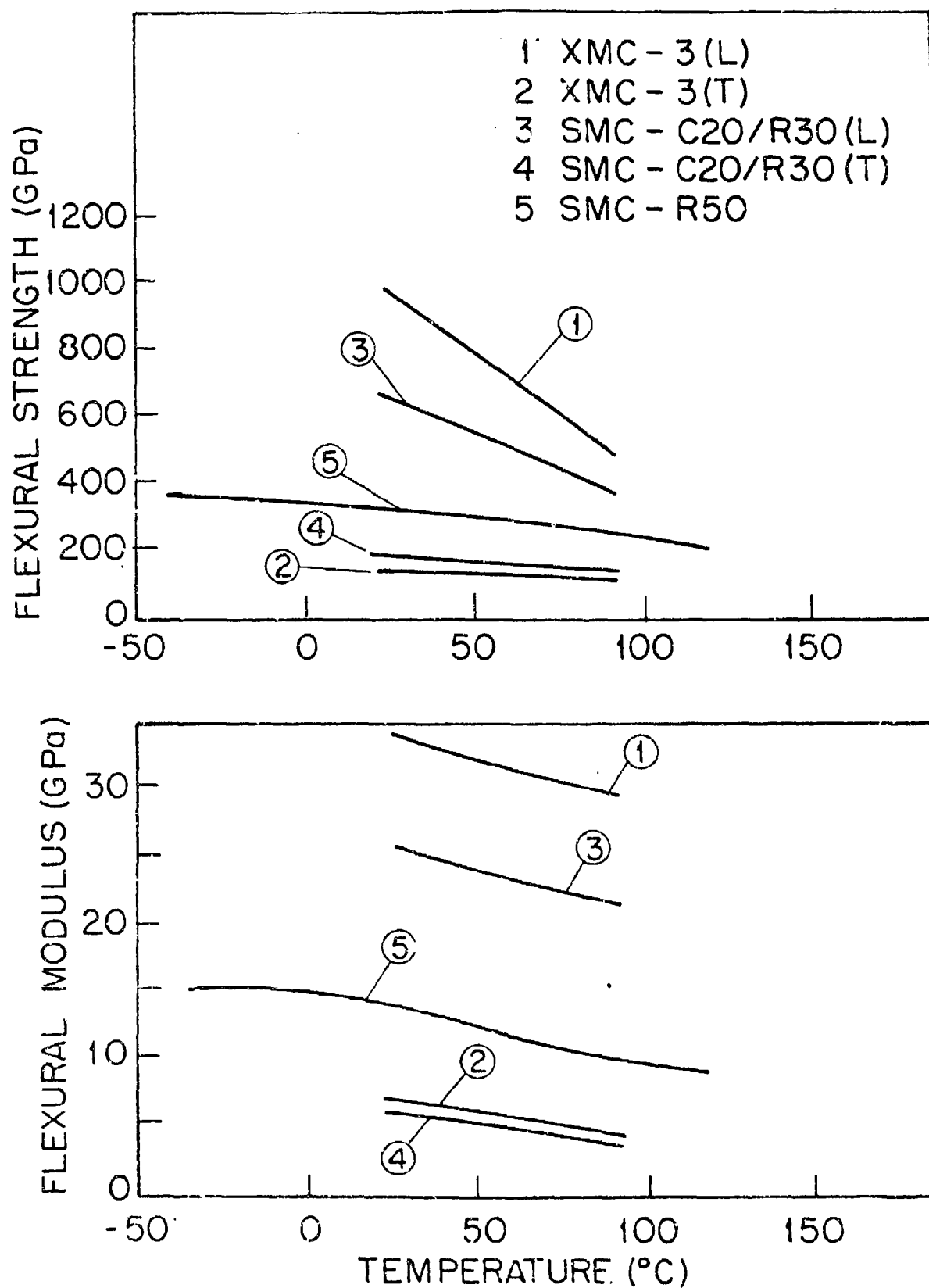


Figure 10: The effect of temperature on the flexural strength and flexural modulus. (L -longitude, T -transverse direction) (ref. 3)

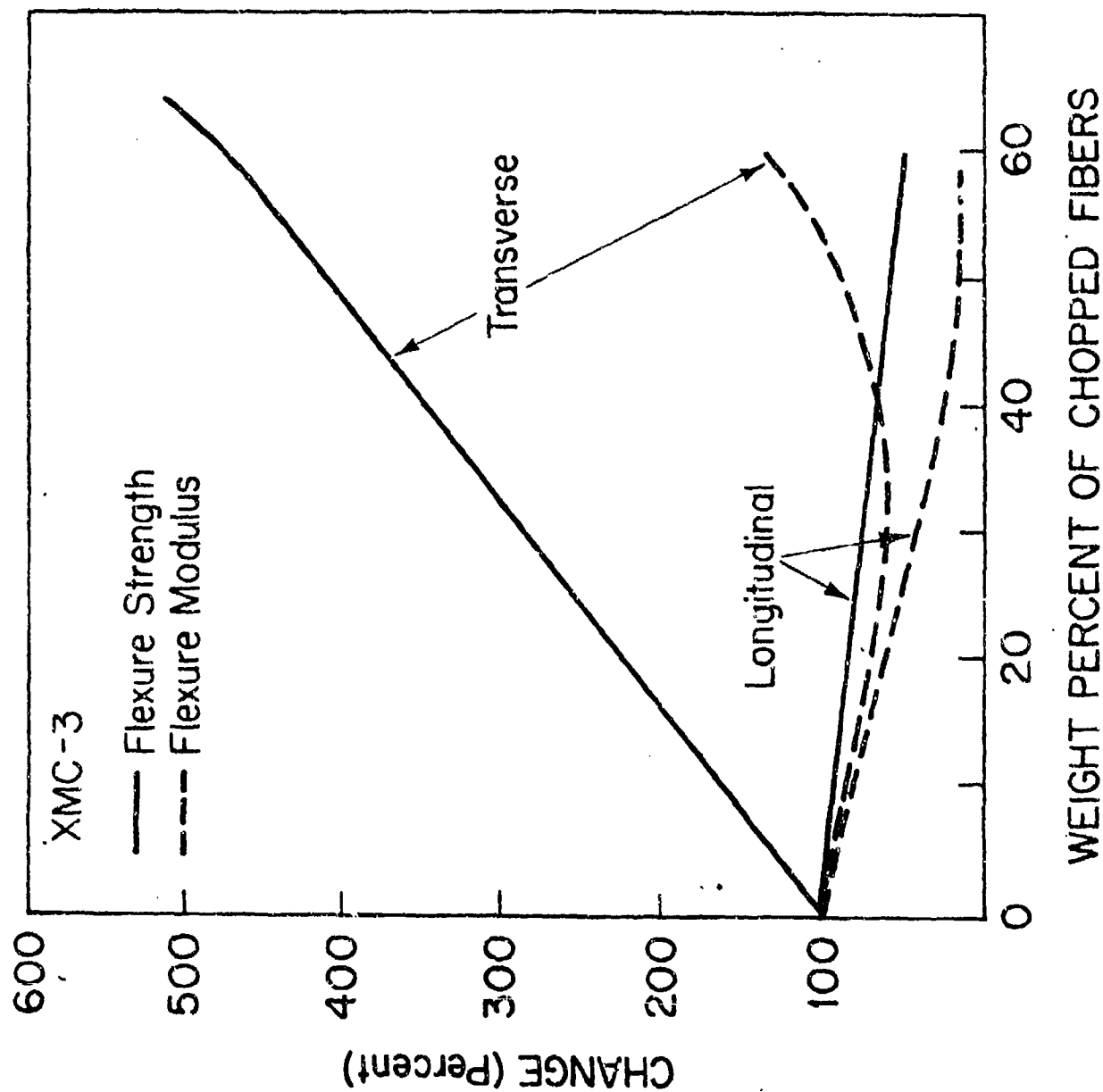


Figure 11: The effect of the amount of chopped fibers on the flexural strength and flexural modulus of XMC-3 composites. Total fiber content by weight = 10 percent (ref. 7).

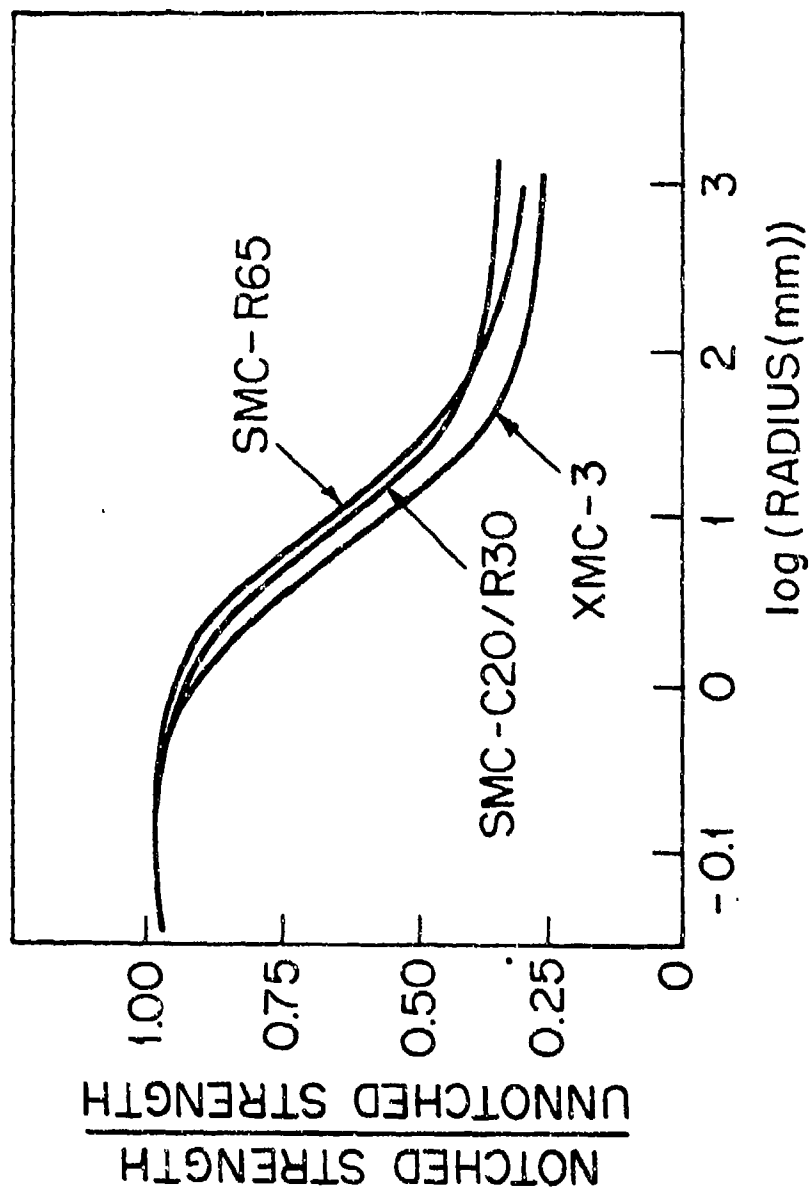


Figure 12: Changes in tensile strengths due to different diameter circular holes ("notches") (ref. 3)

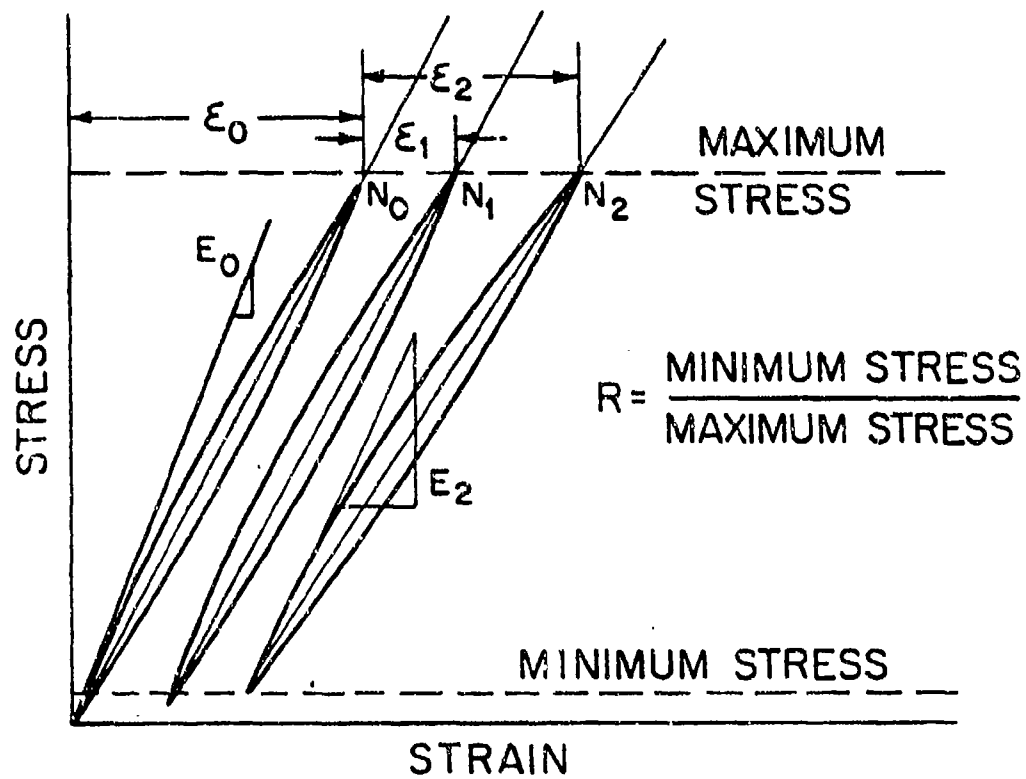


Figure 13: Typical result of fatigue test and definition of symbols used in the presentation of the fatigue results.

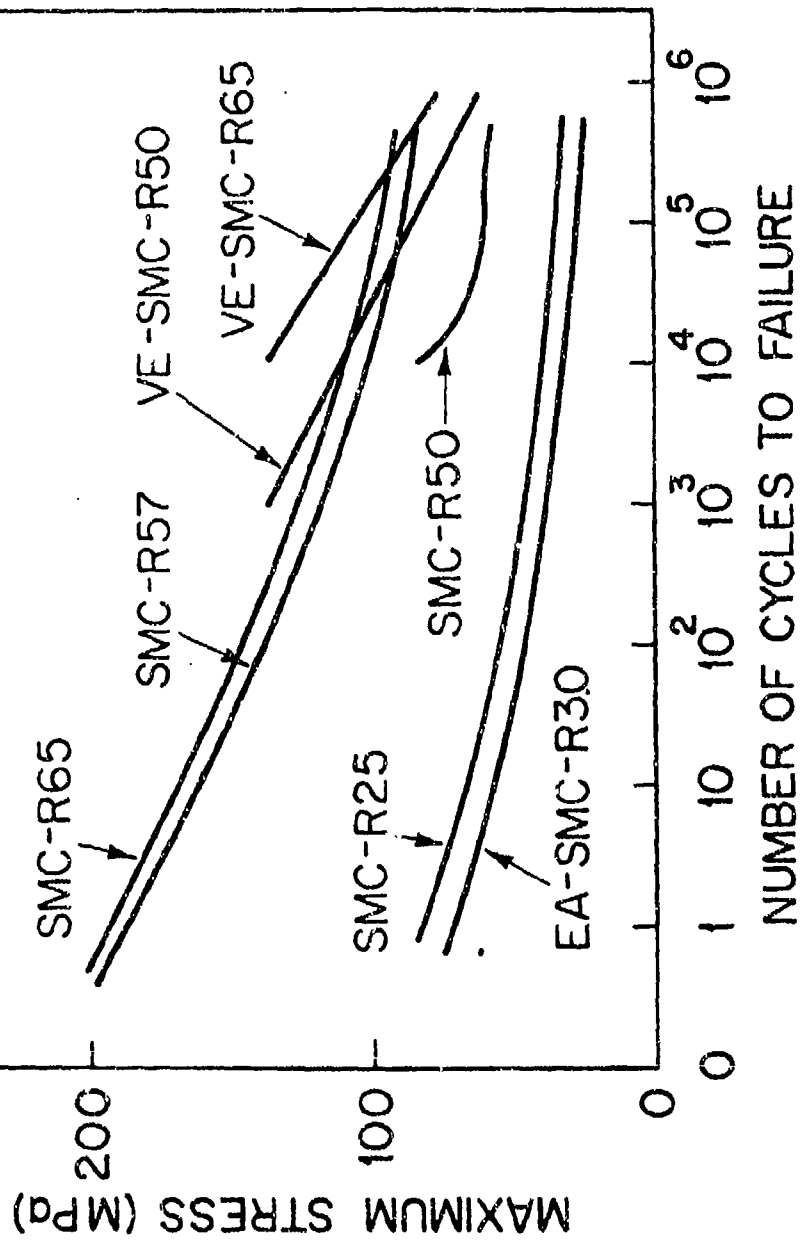


Figure 14: Tension-tension fatigue results. $R = 0.05$ (except for VE-SMC-R50 and VE-SMC-R65) (refs. 2, 5, 6).

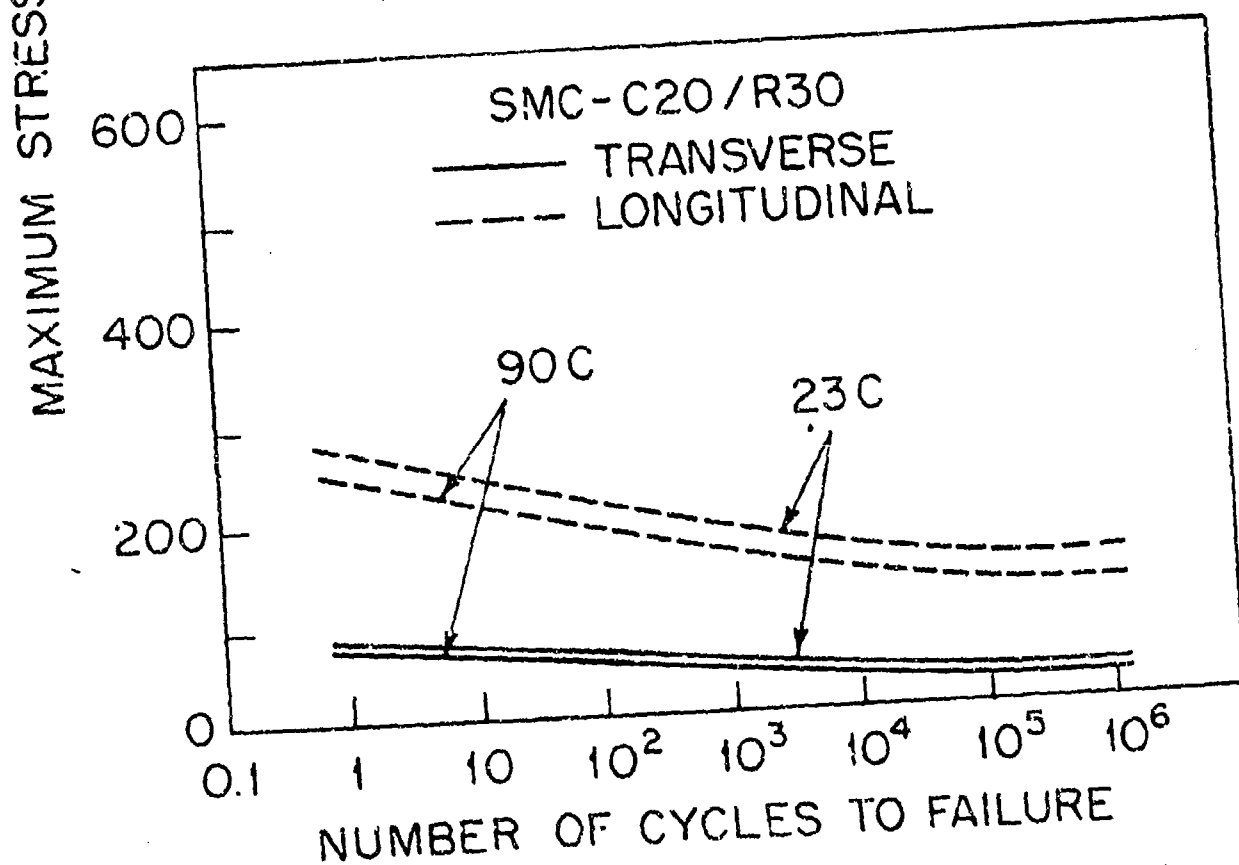
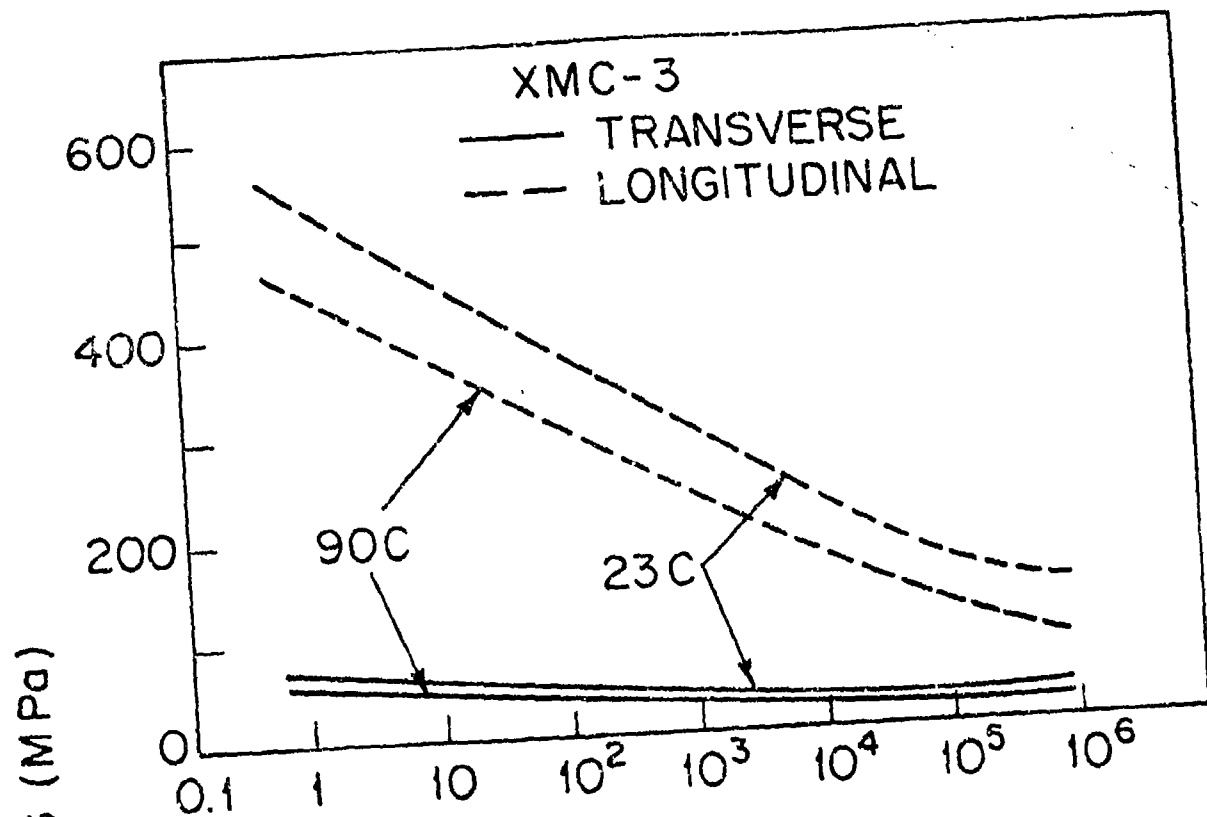


Figure 15: Tension-tension fatigue results. $R = 0.05$ (ref. 3)

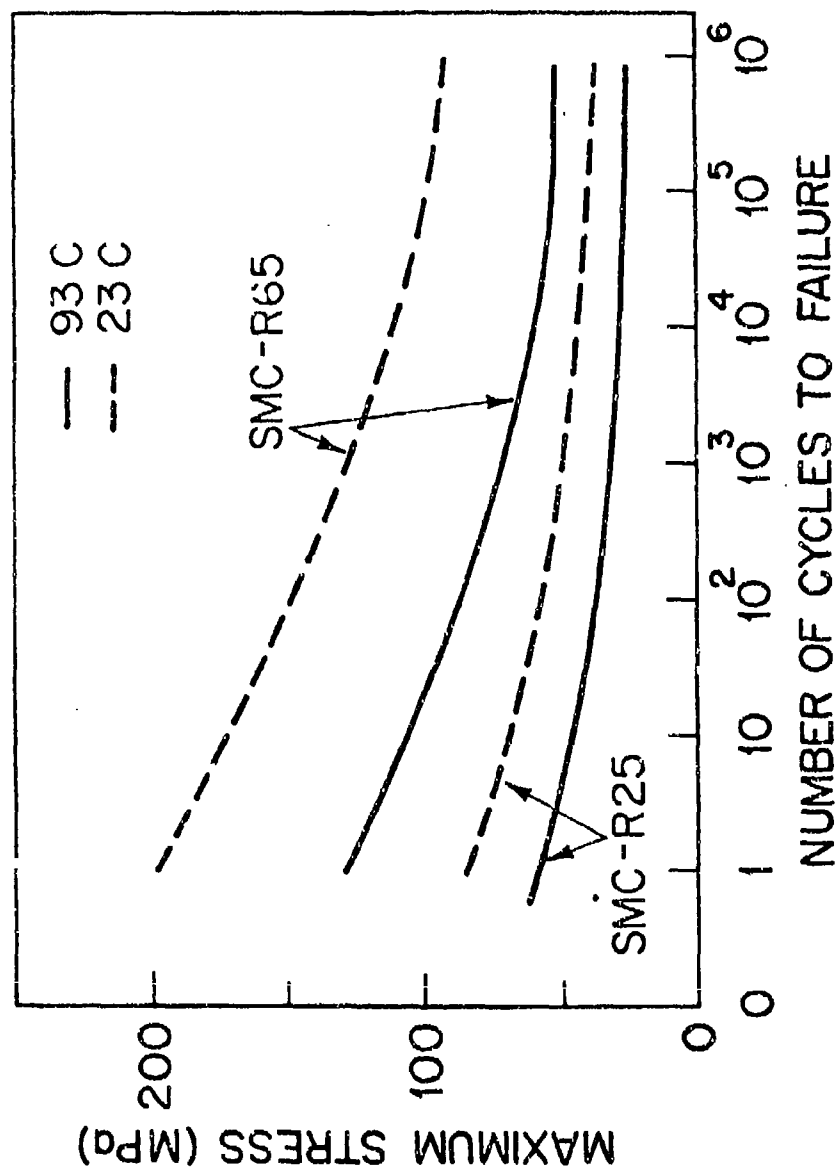


Figure 16: Tension-tension fatigue results. $R = 0.05$ ref. 2)

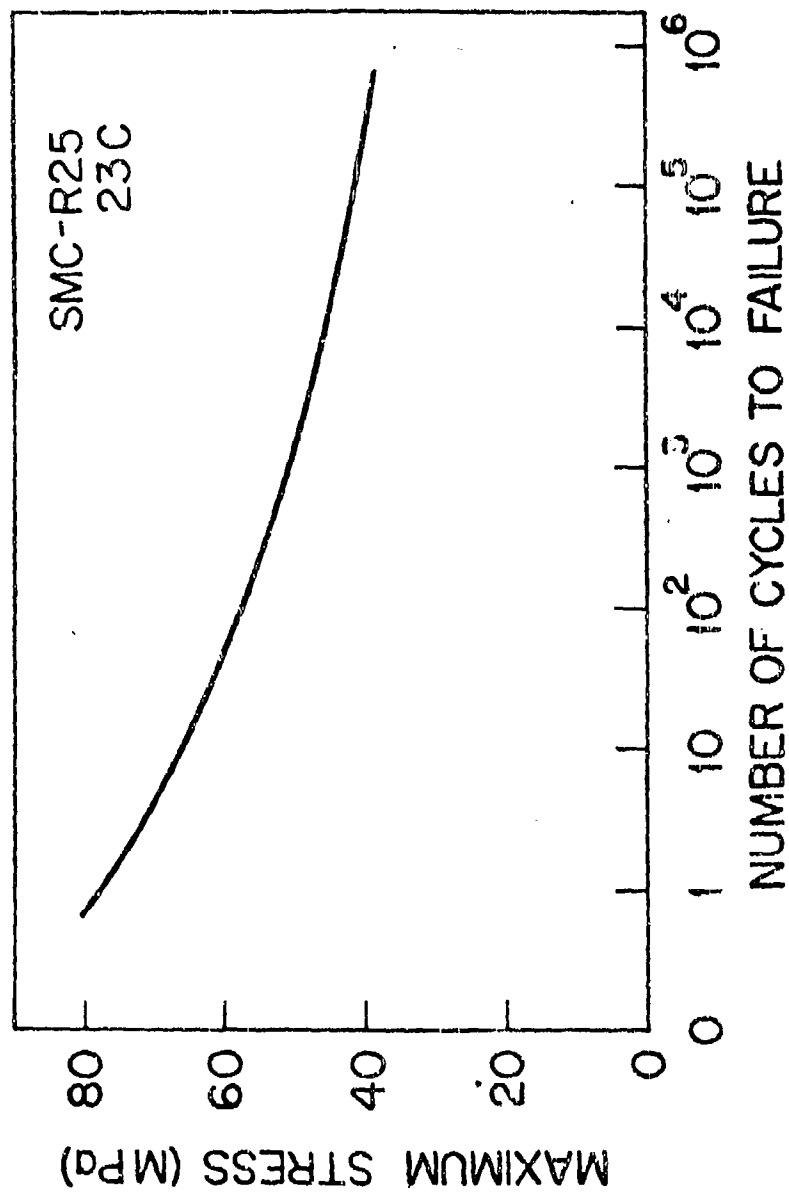


Figure 17: Compression-tension fatigue results. $R = -1$ (ref. 2)

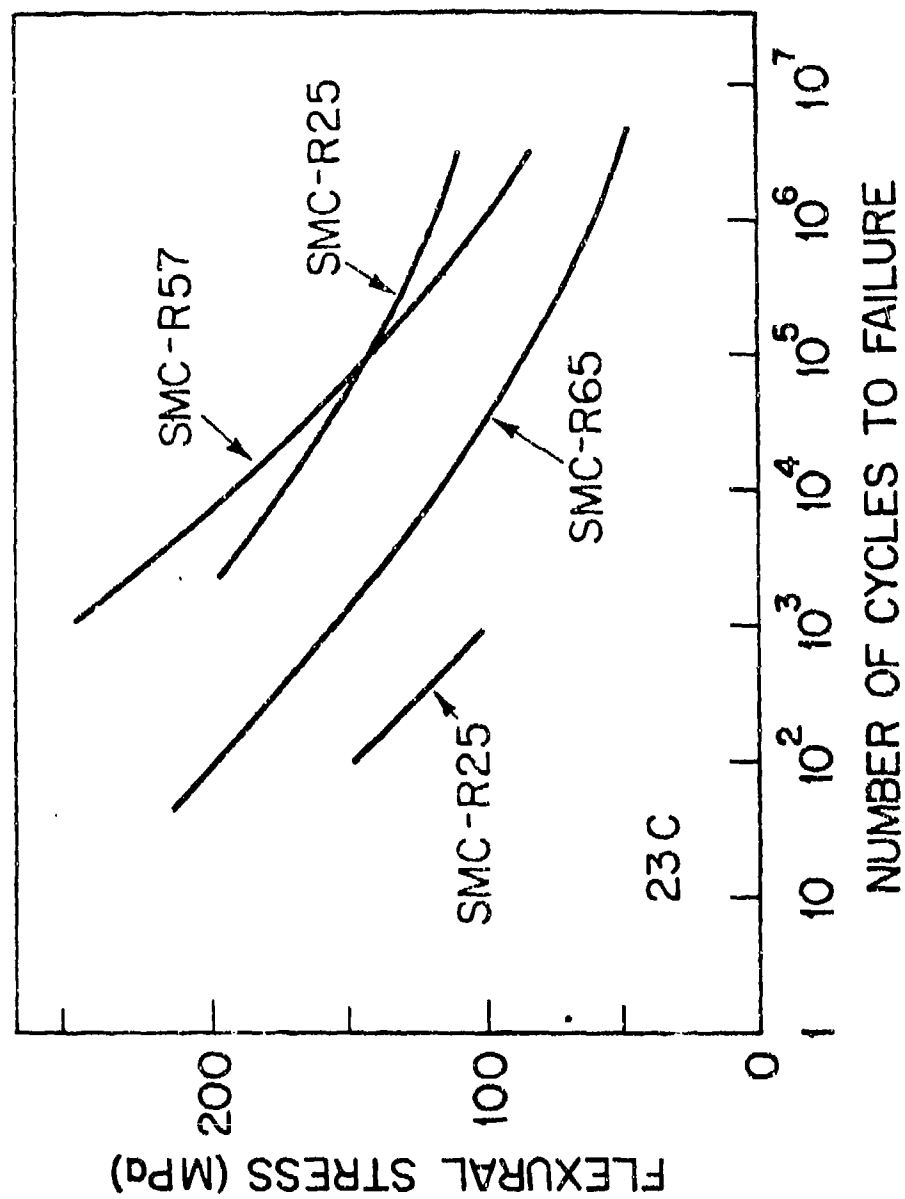


Figure 18: Flexural fatigue results. (ref. 2)

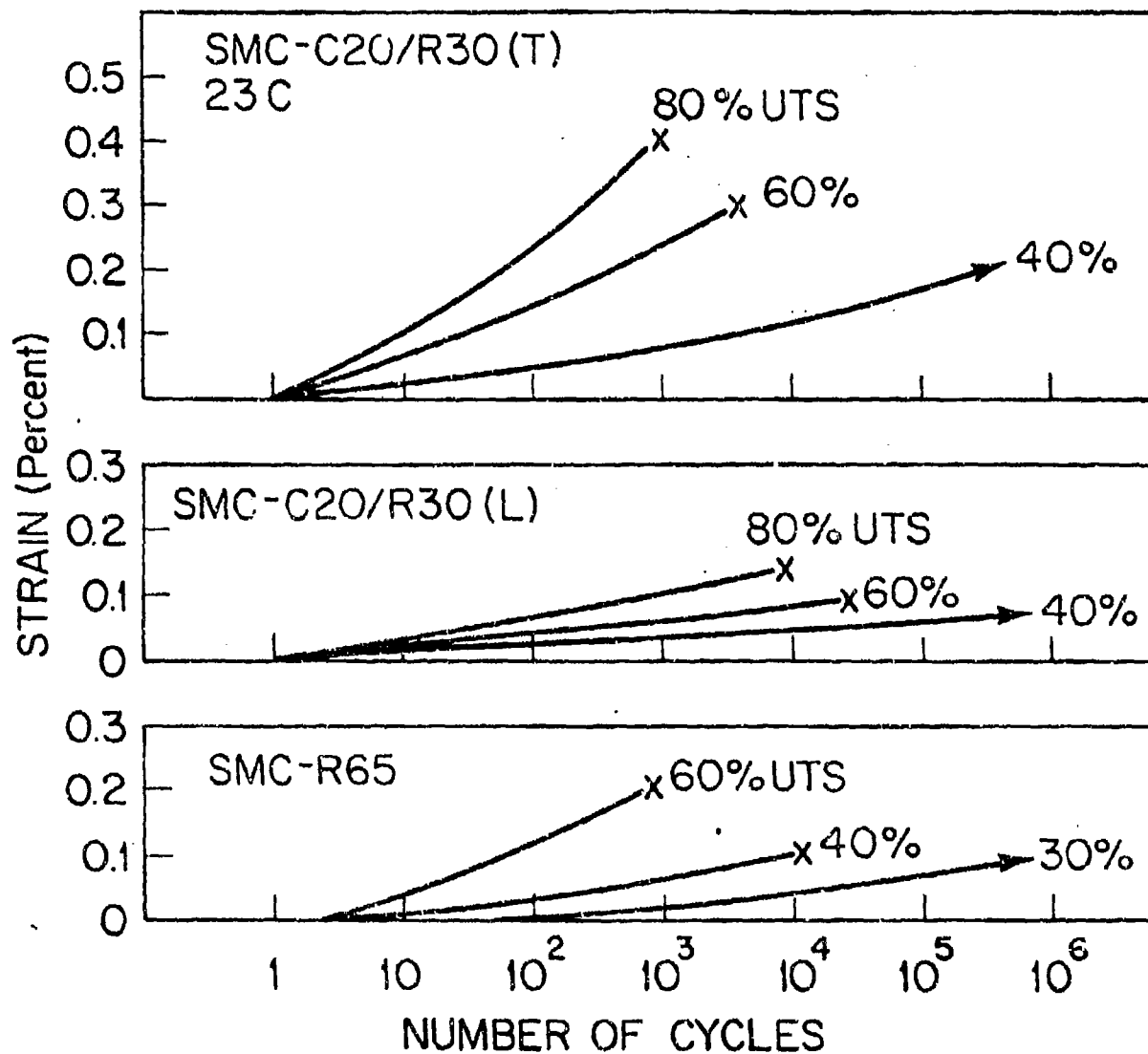


Figure 19: Creep strain ($\epsilon_N - \epsilon_0$) during tension-tension fatigue tests as functions of load (percent of ultimate tensile strength).
 $R = 0.05$ (refs. 2, 3)

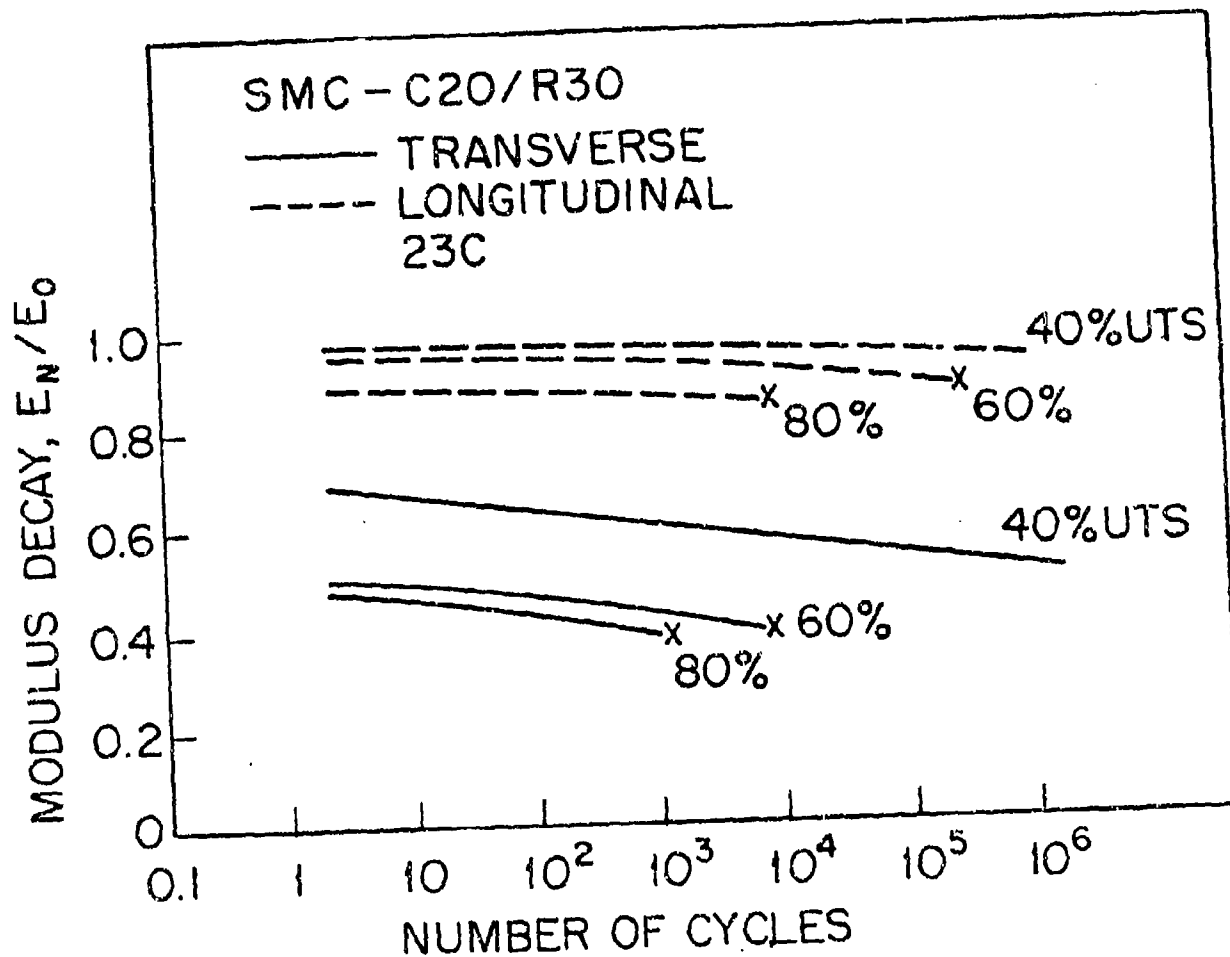


Figure 20: Modulus decay during tension-tension fatigue tests as a function of load (percent of ultimate tensile strength). $R = 0.05$ (ref. 3)

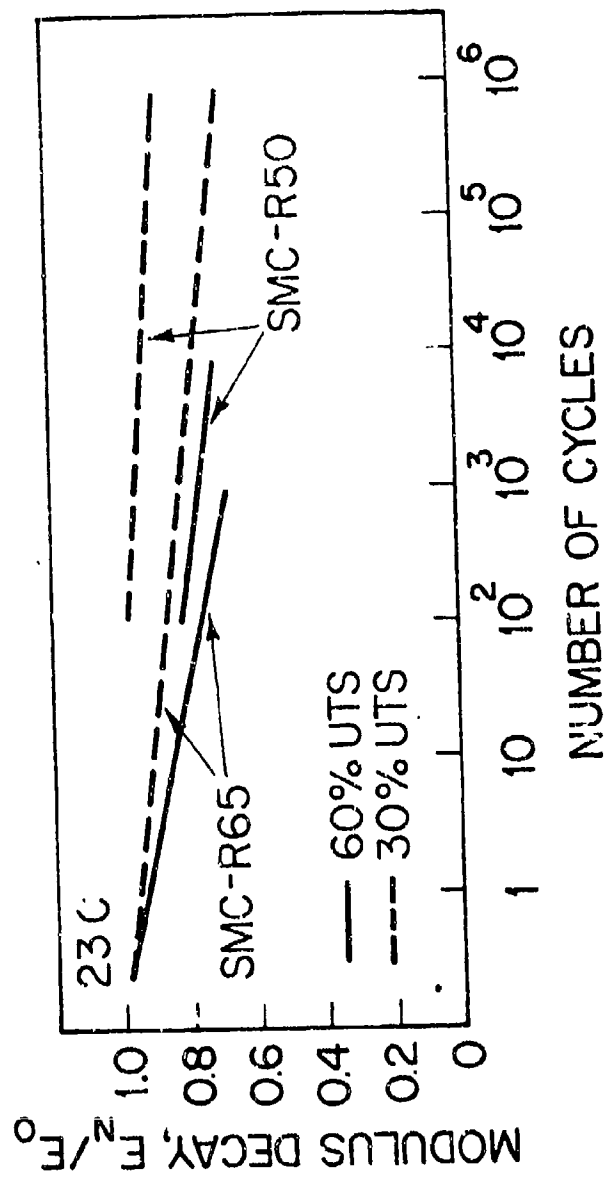


Figure 21: Modulus decay during tension-tension fatigue tests as a function of load (percent of ultimate tensile strength). $R = 0.05$ (refs. 2, 4)

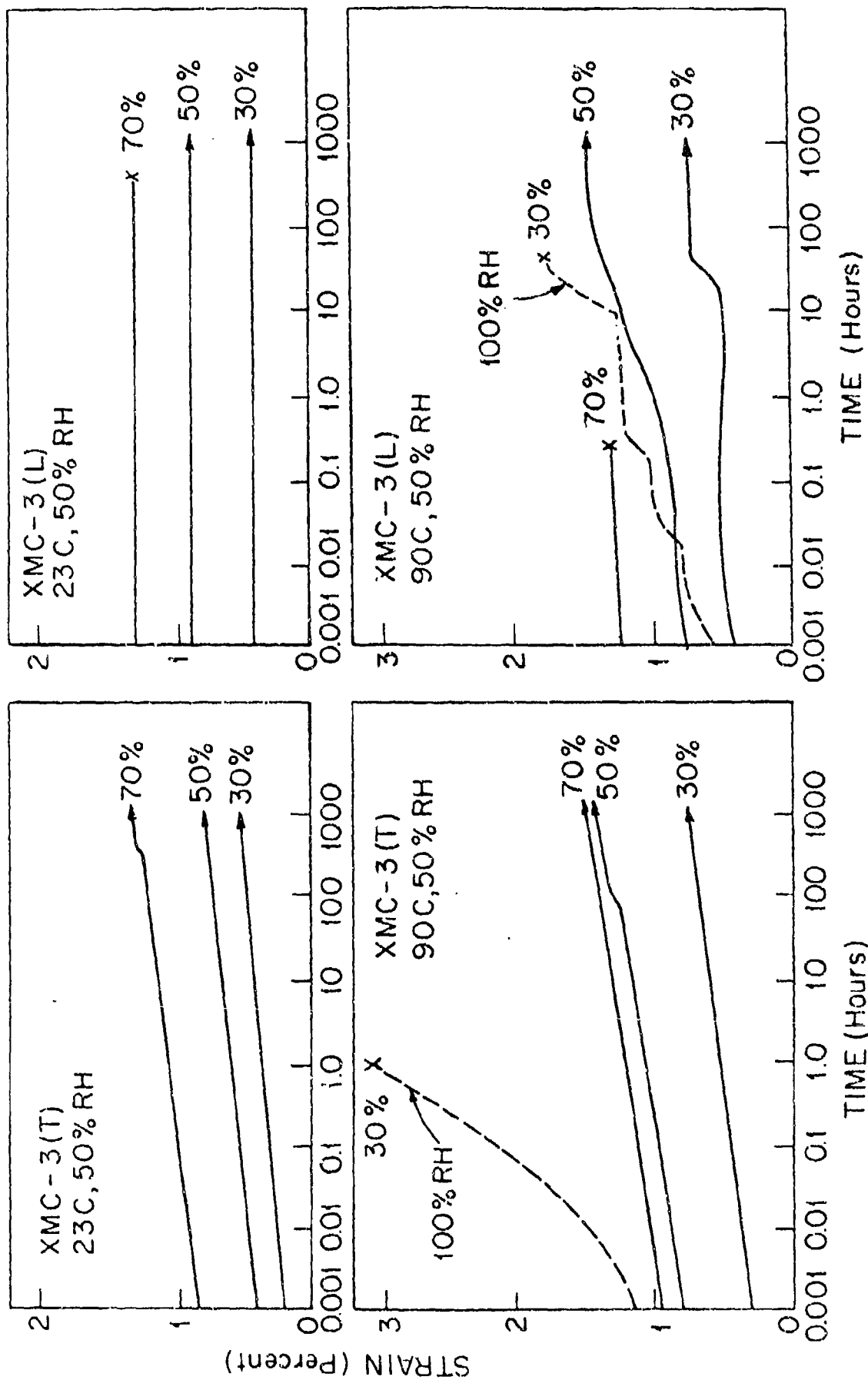


Figure 22: Creep of XMC-3 at 70, 50, and 30 percent of static ultimate tensile strength (L - longitudinal, T - transverse direction) (ref. 3)

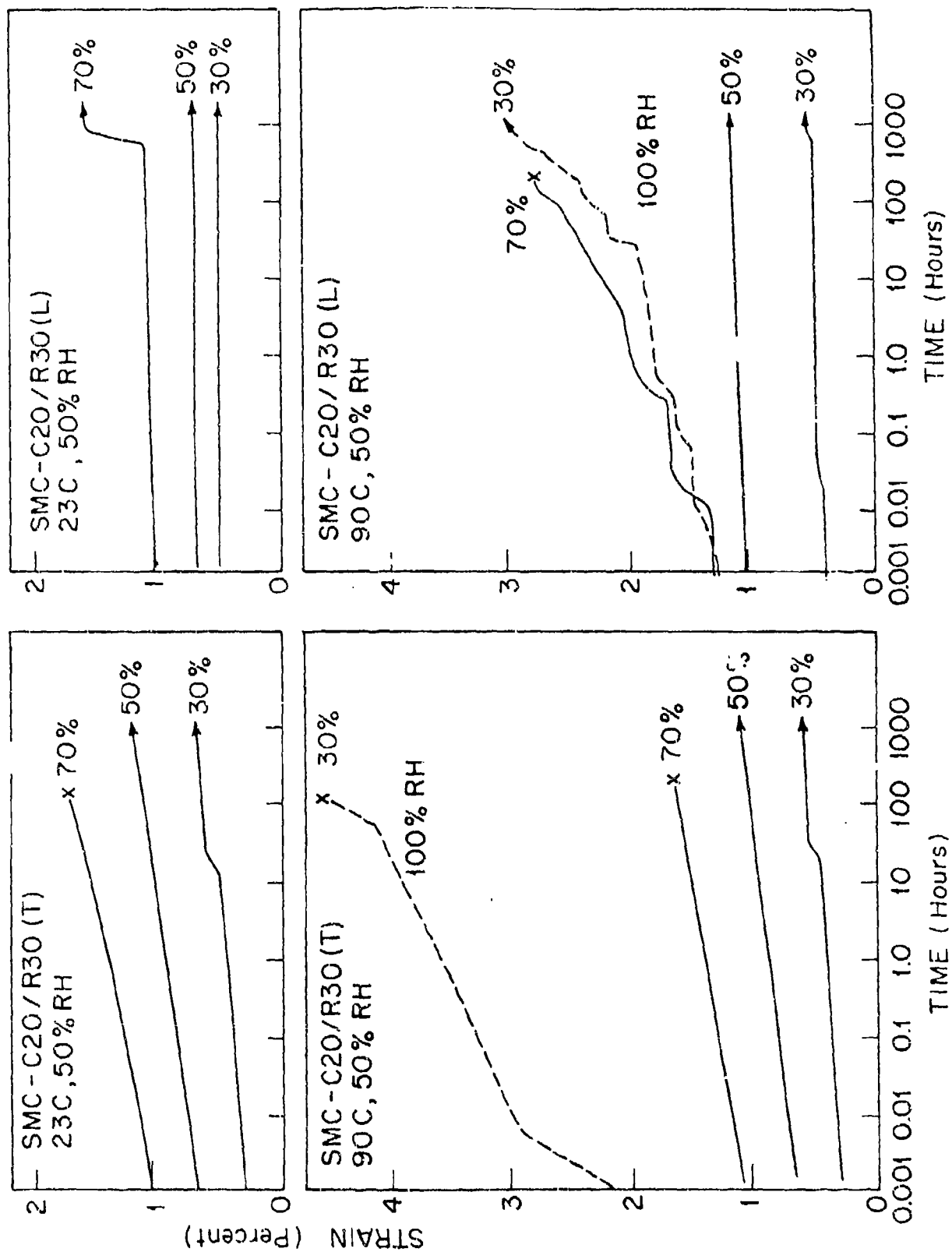


Figure 23: Creep of SMC-C20/R30 at 70, 50 and 30 percent of static ultimate stress. (T - longitudinal, L - transverse direction) (ref. 3)

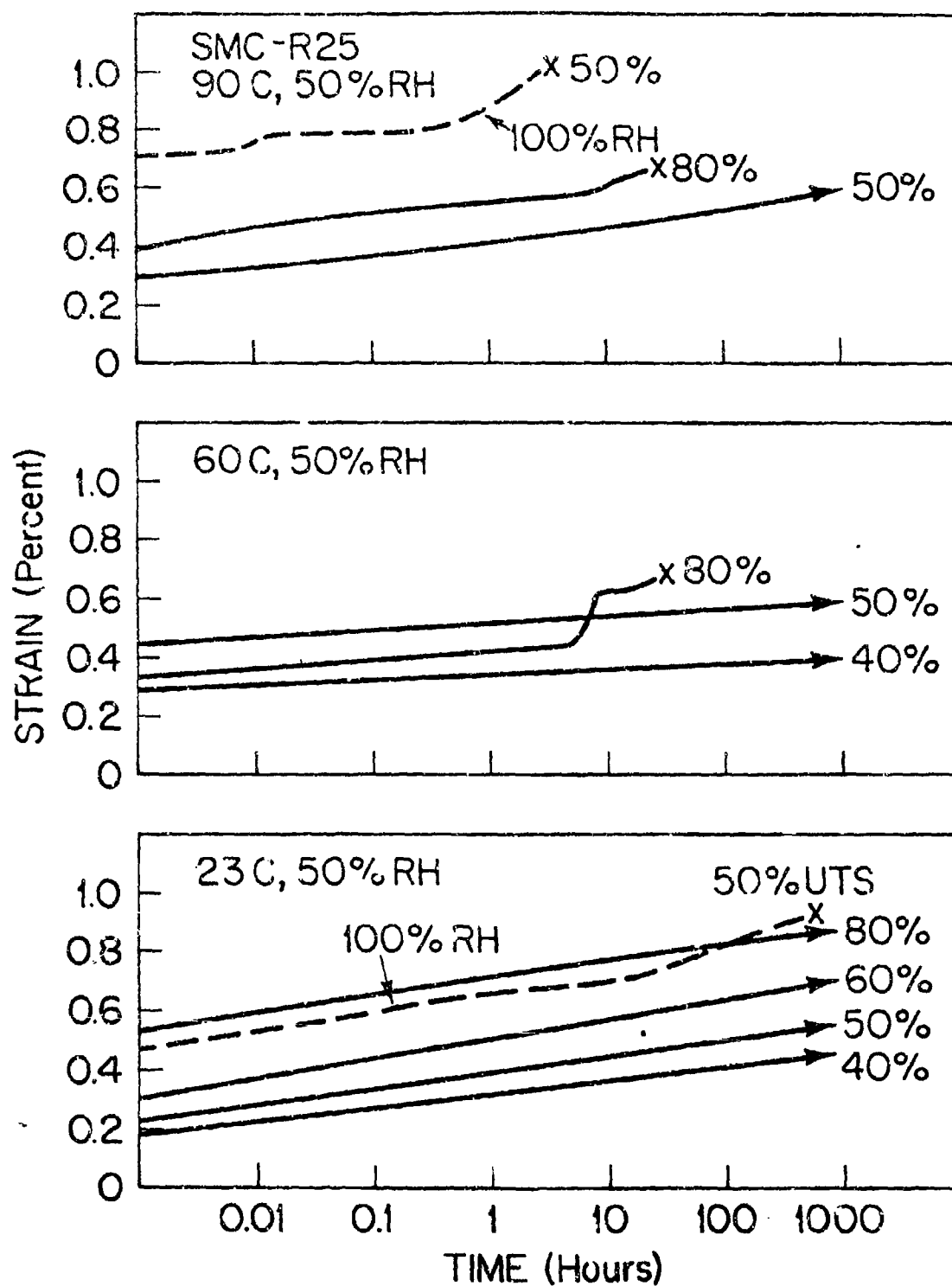


Figure 24: Creep of SMC-R25 under different loads (percent of static ultimate tensile strength (ref. 2))

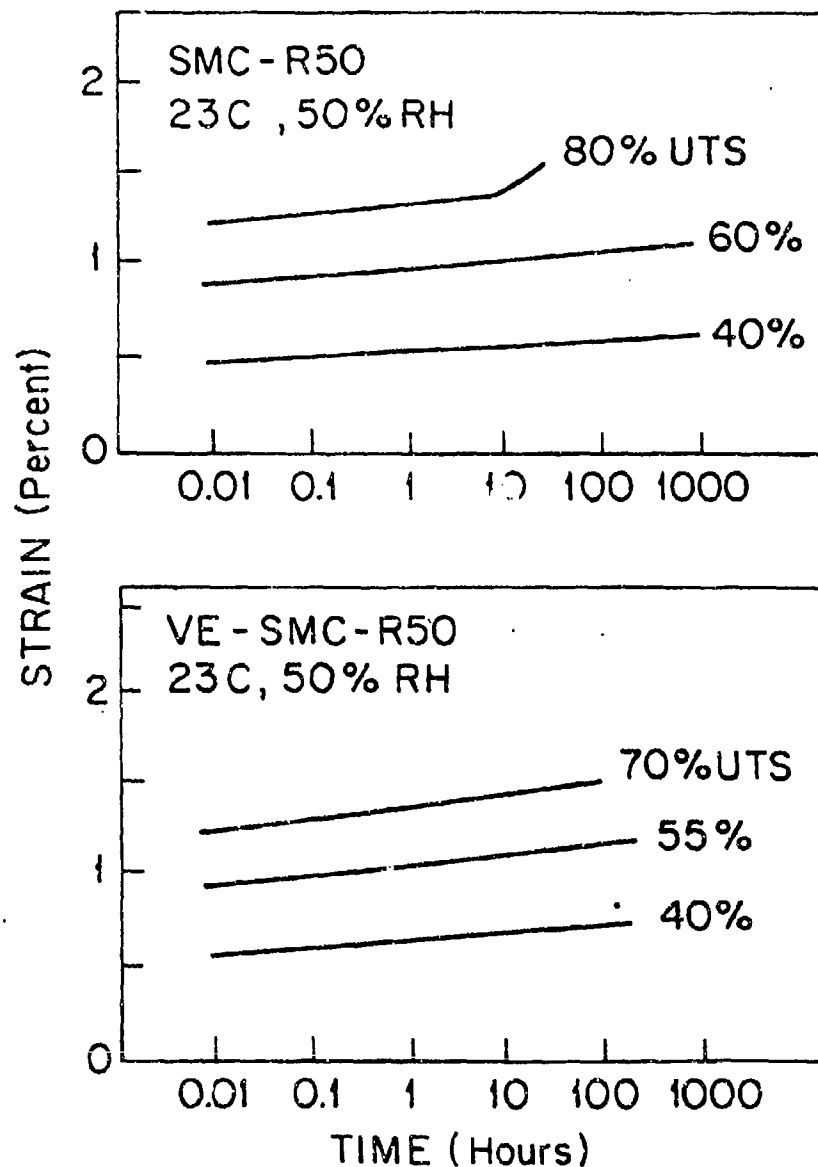


Figure 25: Creep of SMC-R50 and VE-SMC-R50 under different loads (percent of static ultimate tensile strength) (refs. 5, 6)

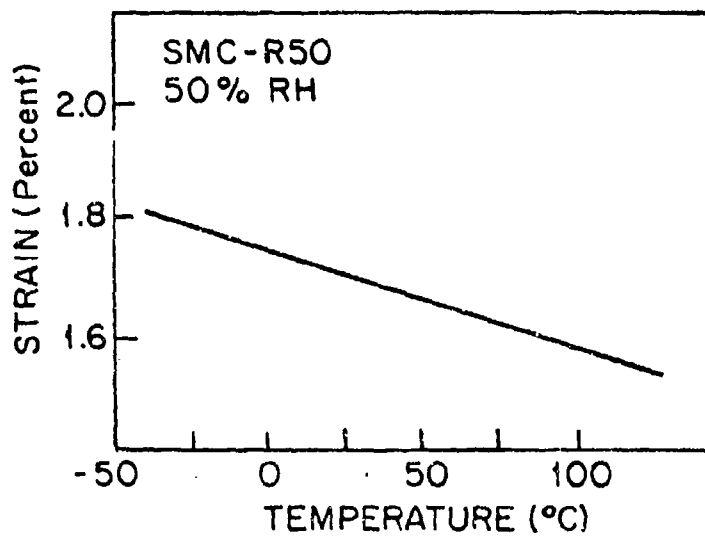


Figure 26: Strain (elongation) of SMC-R50 at failure as a function of temperature (ref. 5)

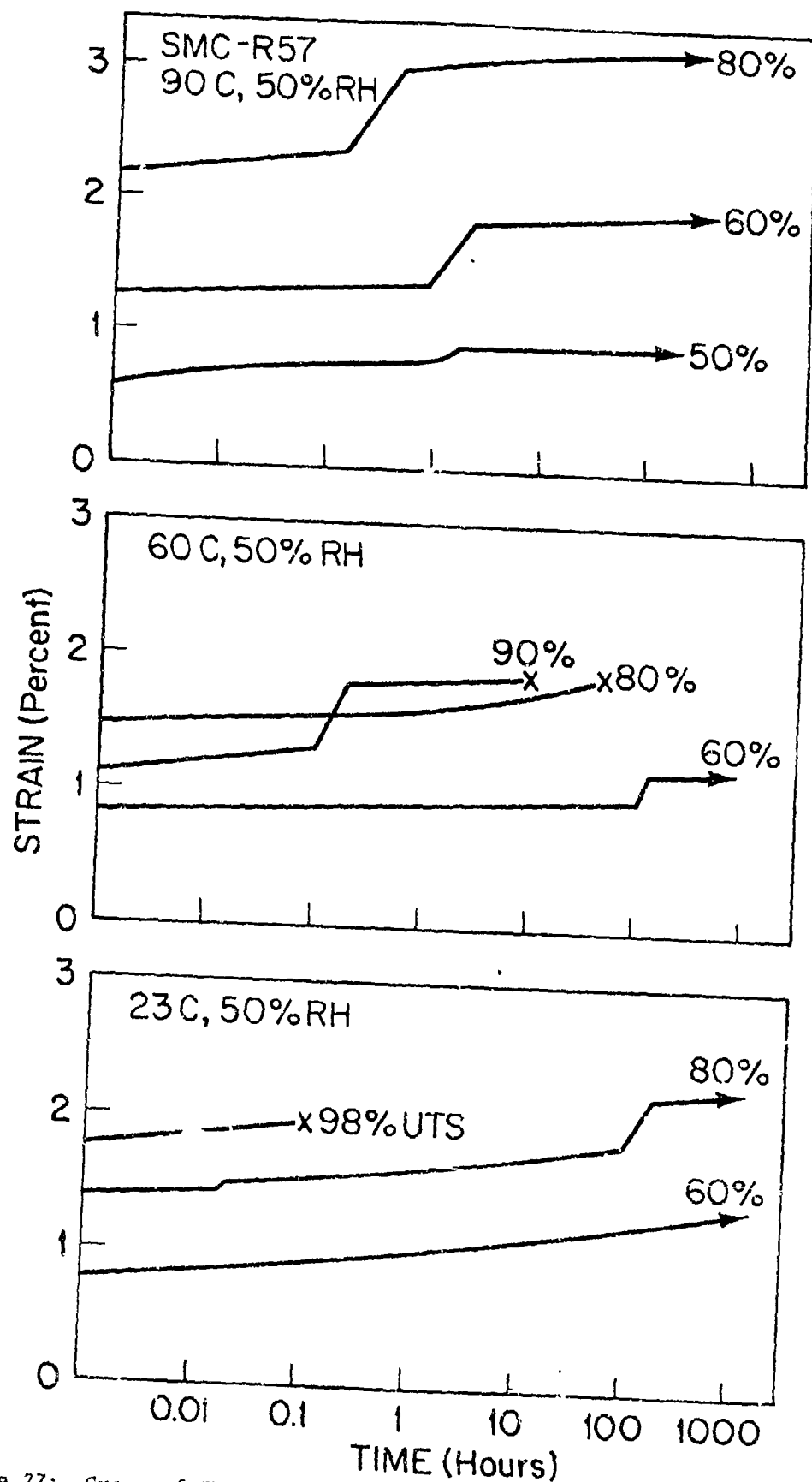


Figure 27: Creep of SMC-R57 under different loads (percent of static ultimate tensile strength) (ref. 2)

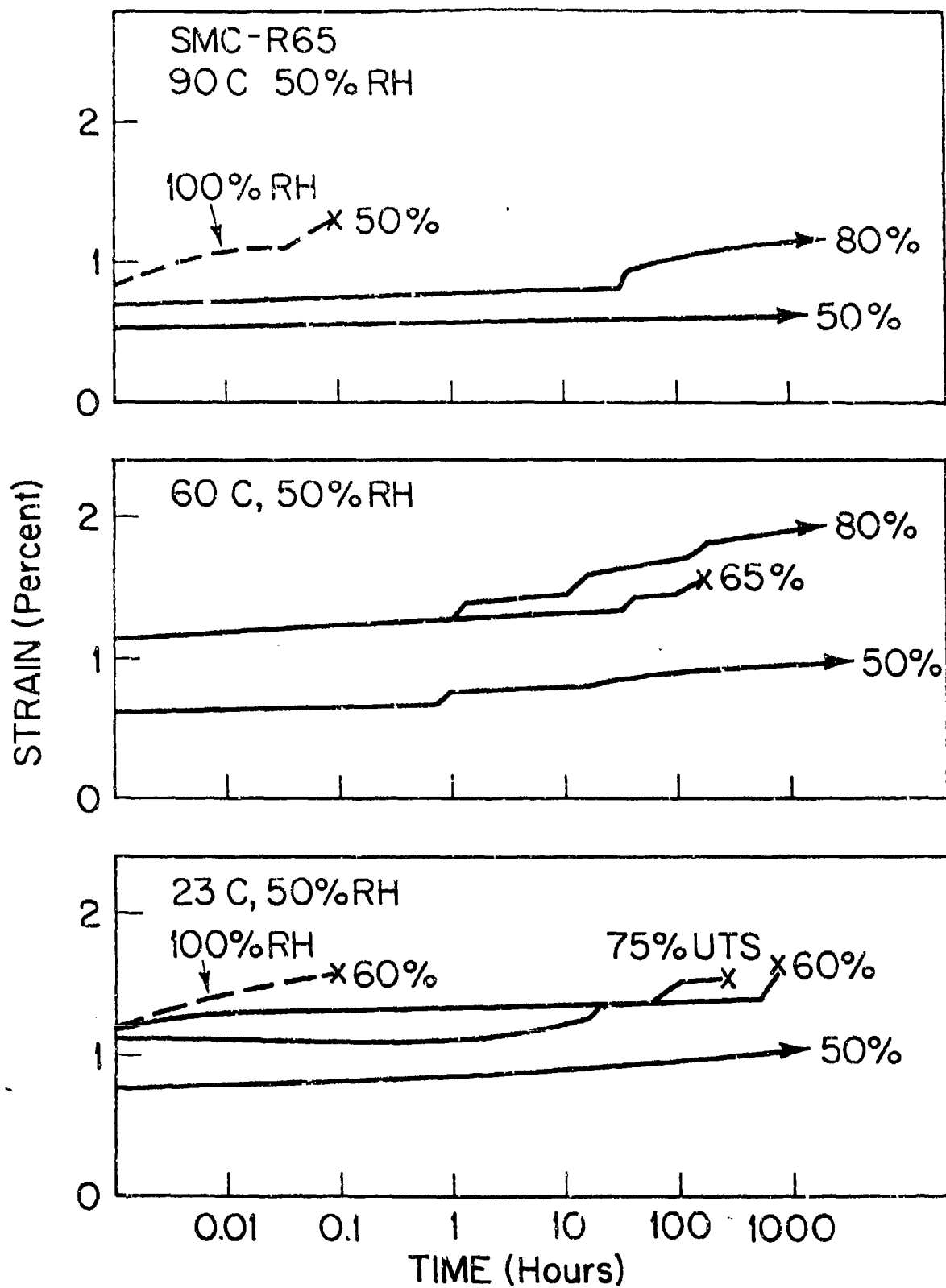


Figure 28: Creep of SMC-R65 under different loads (percent of static ultimate tensile strength (ref. 2))

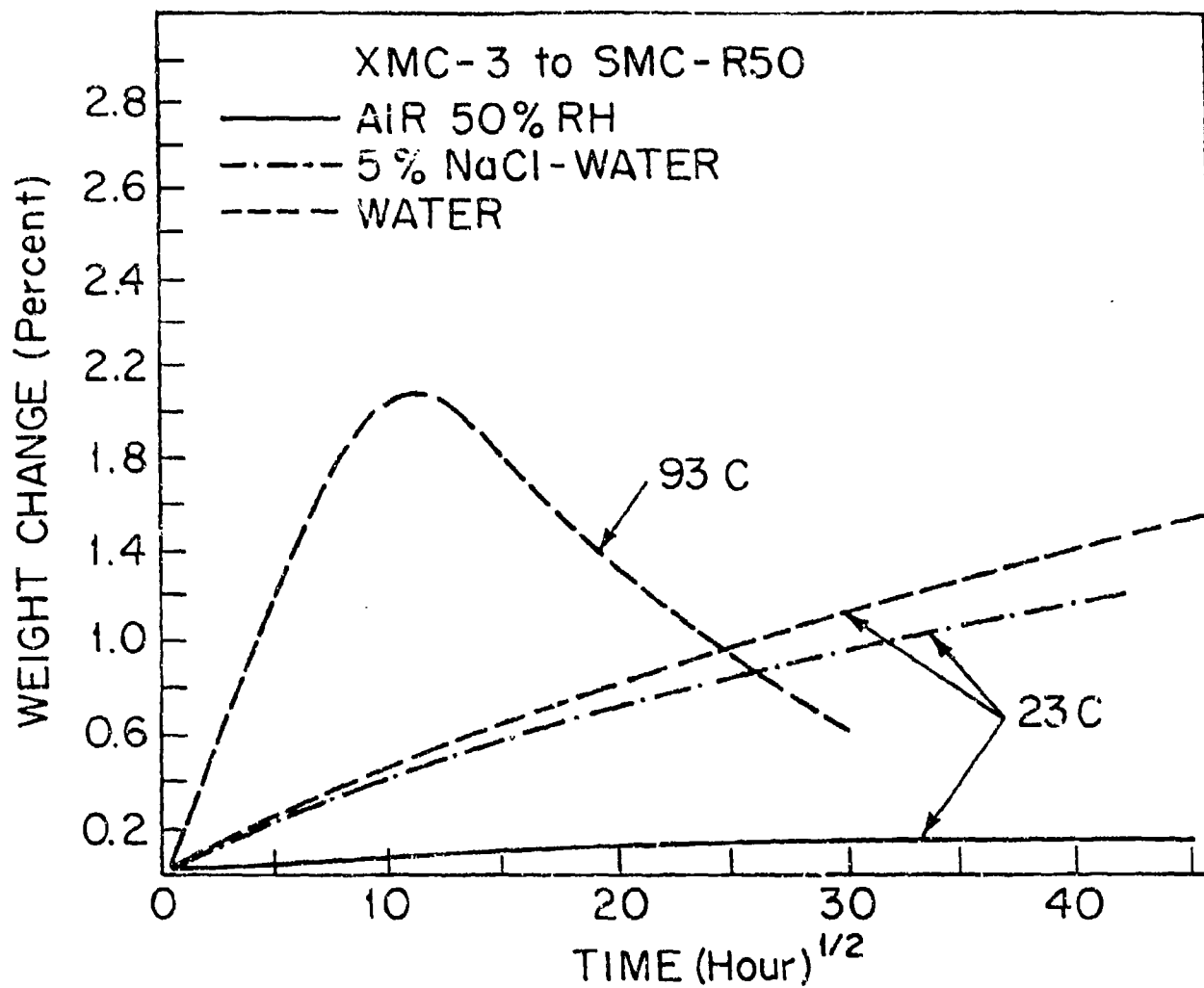


Figure 29: Moisture absorption of adhesive bonded XMC-3 to SMC-R50 single lap joints

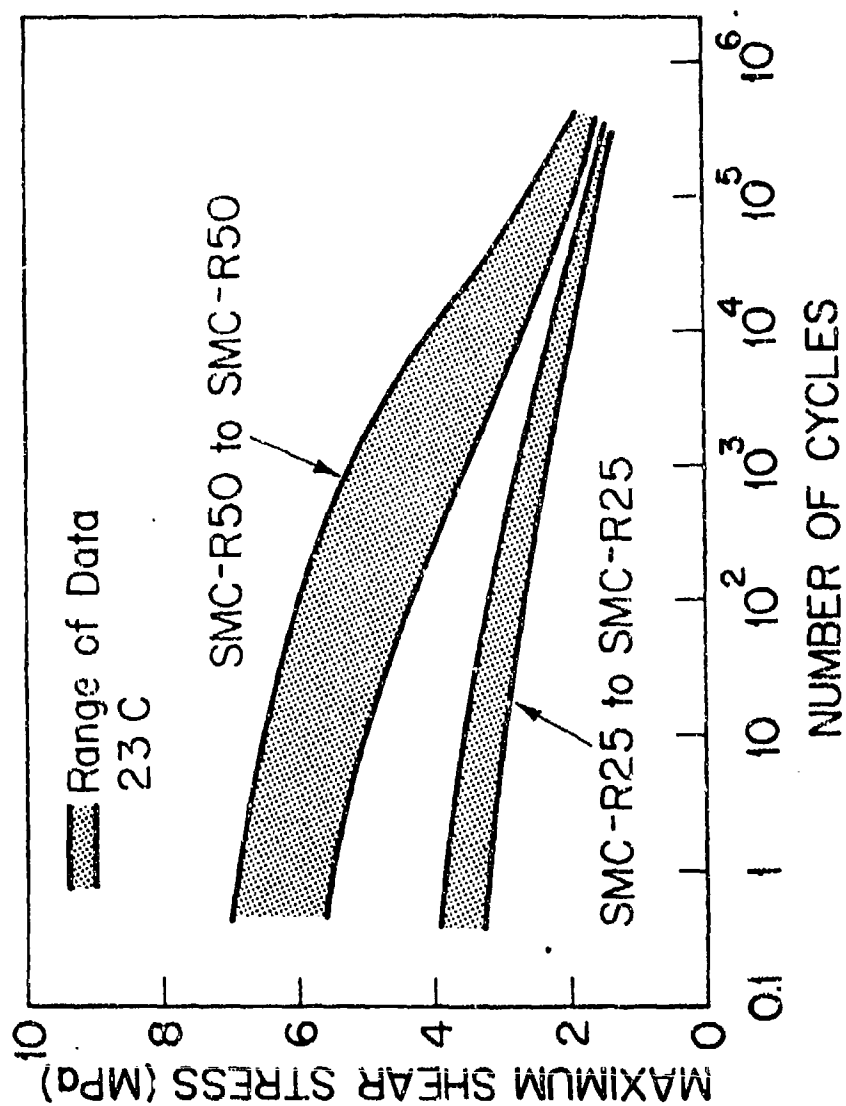


Figure 30: Maximum shear stress of adhesive bonded single lap joints (SMC-R50 to SMC-R50 and SMC-R25 to SMC-R25) during tension-tension fatigue (ref. 11)

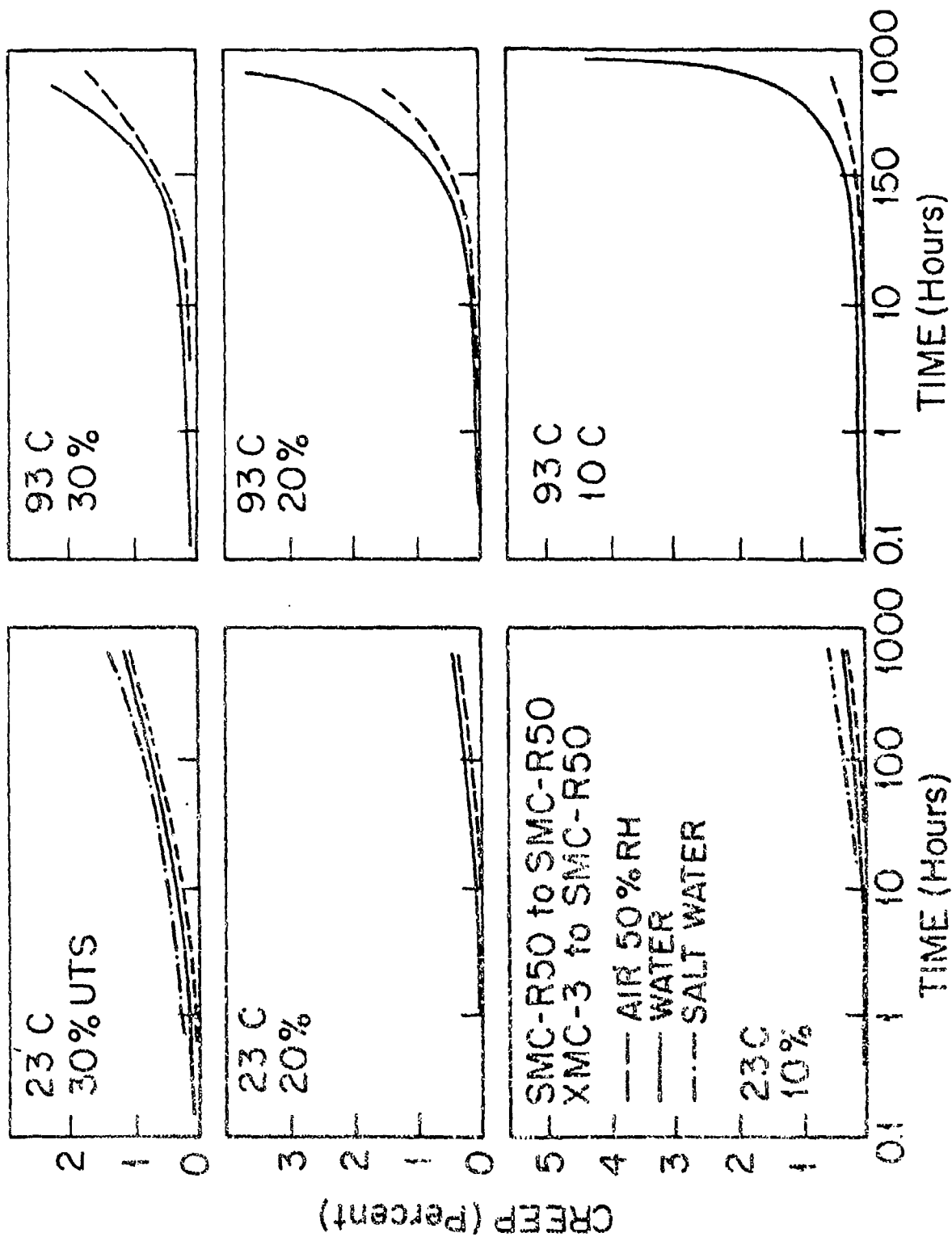


Figure 31: Creep of adhesive bonded single lap joints (SMC-R50 to SMC-R50 and XMC-3 to SMC-R50) immersed in air, water, and 5% NaCl-water mixture under different loads (percent of static ultimate tensile strength)

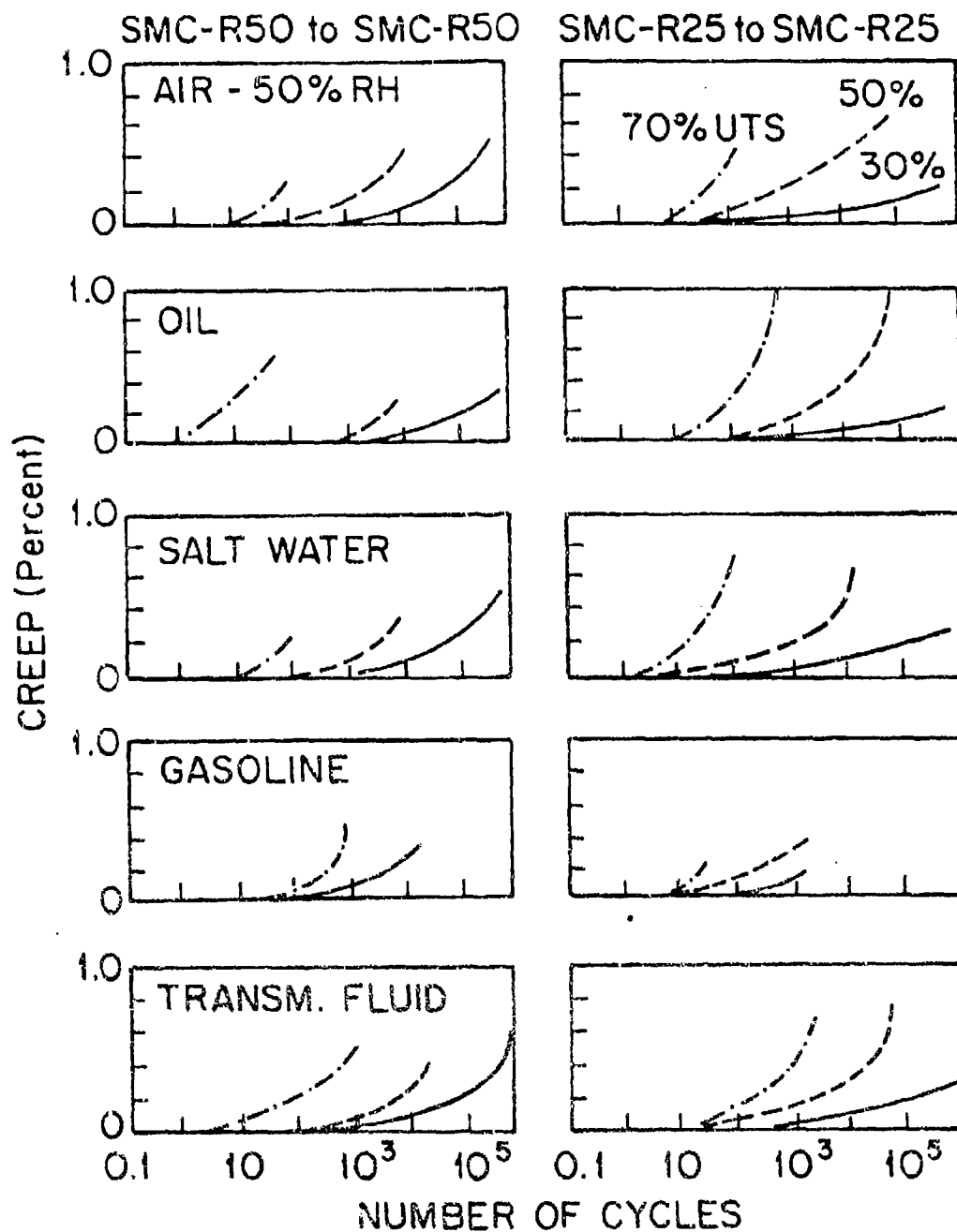


Figure 32: Creep of adhesive bonded single lap joints (SMC-R50 to SMC-R50 and SMC-R25 to SMC-R25) during tension-tension fatigue under different loads (---30% UTS, ----50% UTS, -.-70% UTS) (ref. 11)

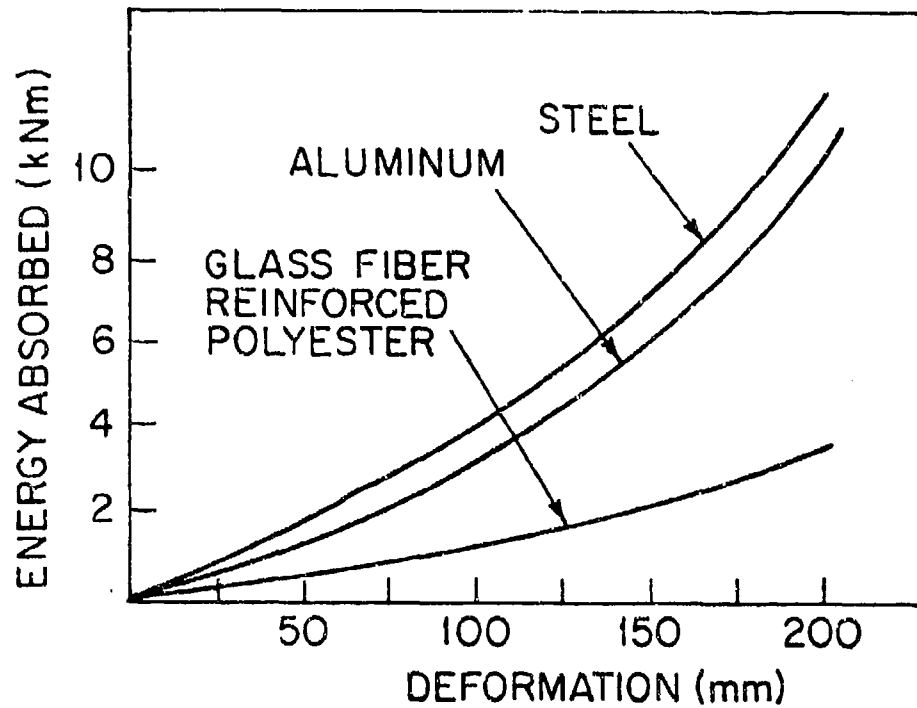


Figure 33: Energy absorbed by different materials during impact against a fixed barrier. Impact speed 24 km/h (ref. 13)

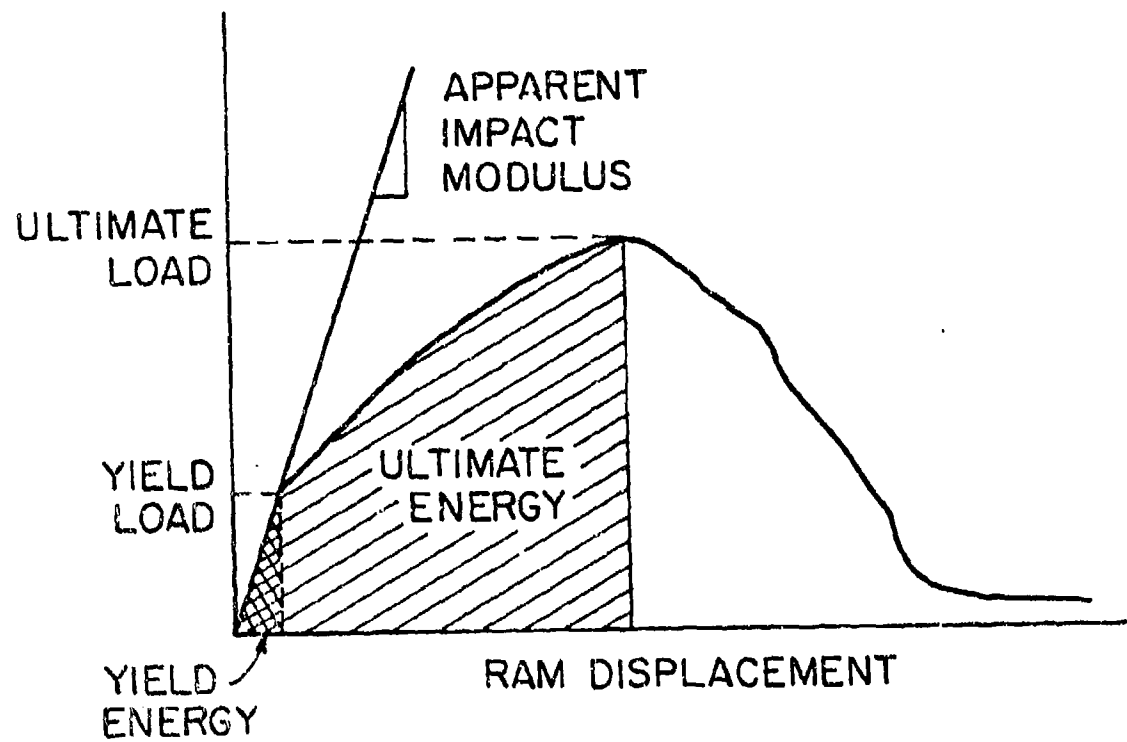


Figure 34: Typical output of impact test using Rheometrics impact tester (ref. 3)

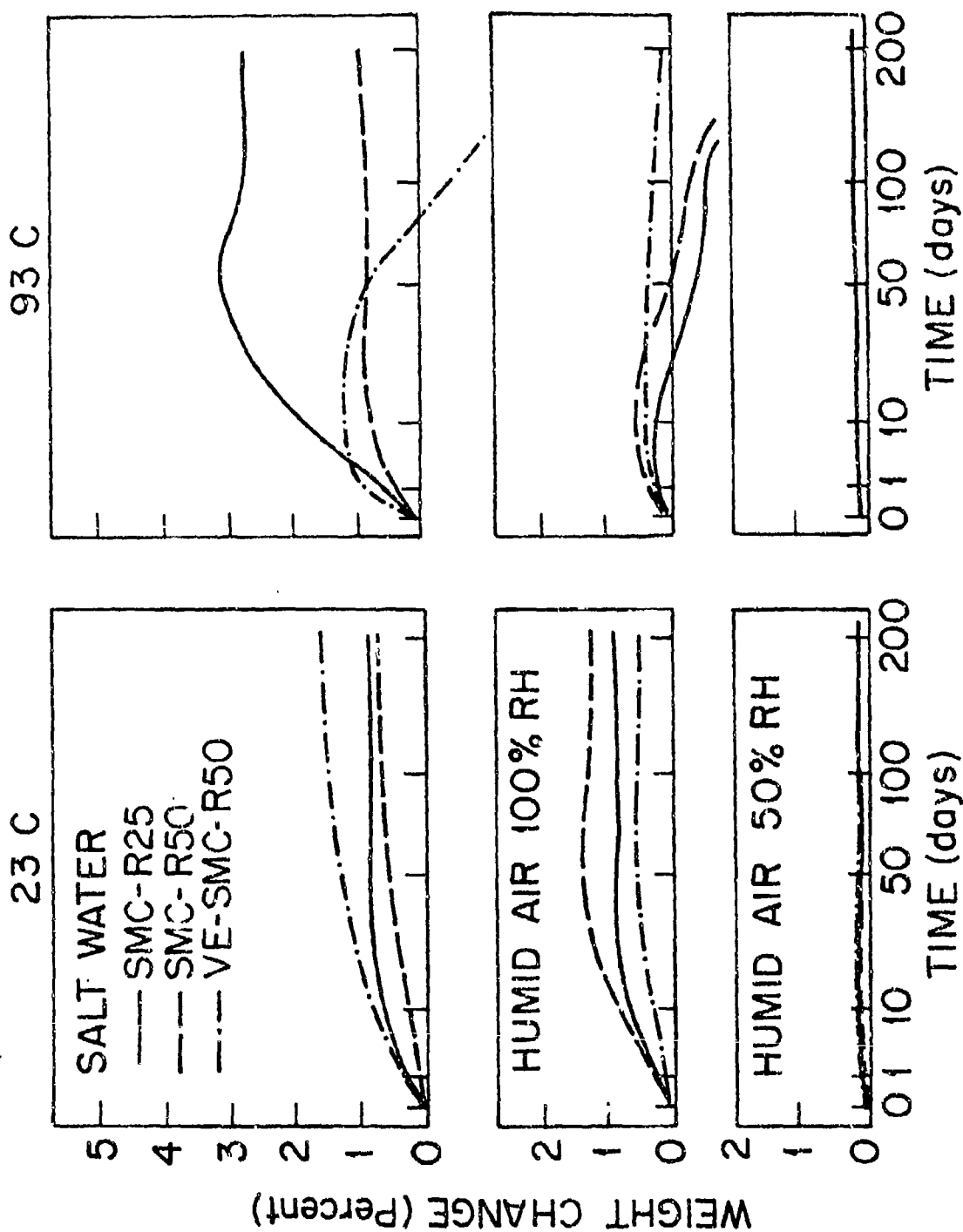


Figure 35: Weight change during immersion in humid air and in saturated salt water (ref. 4)

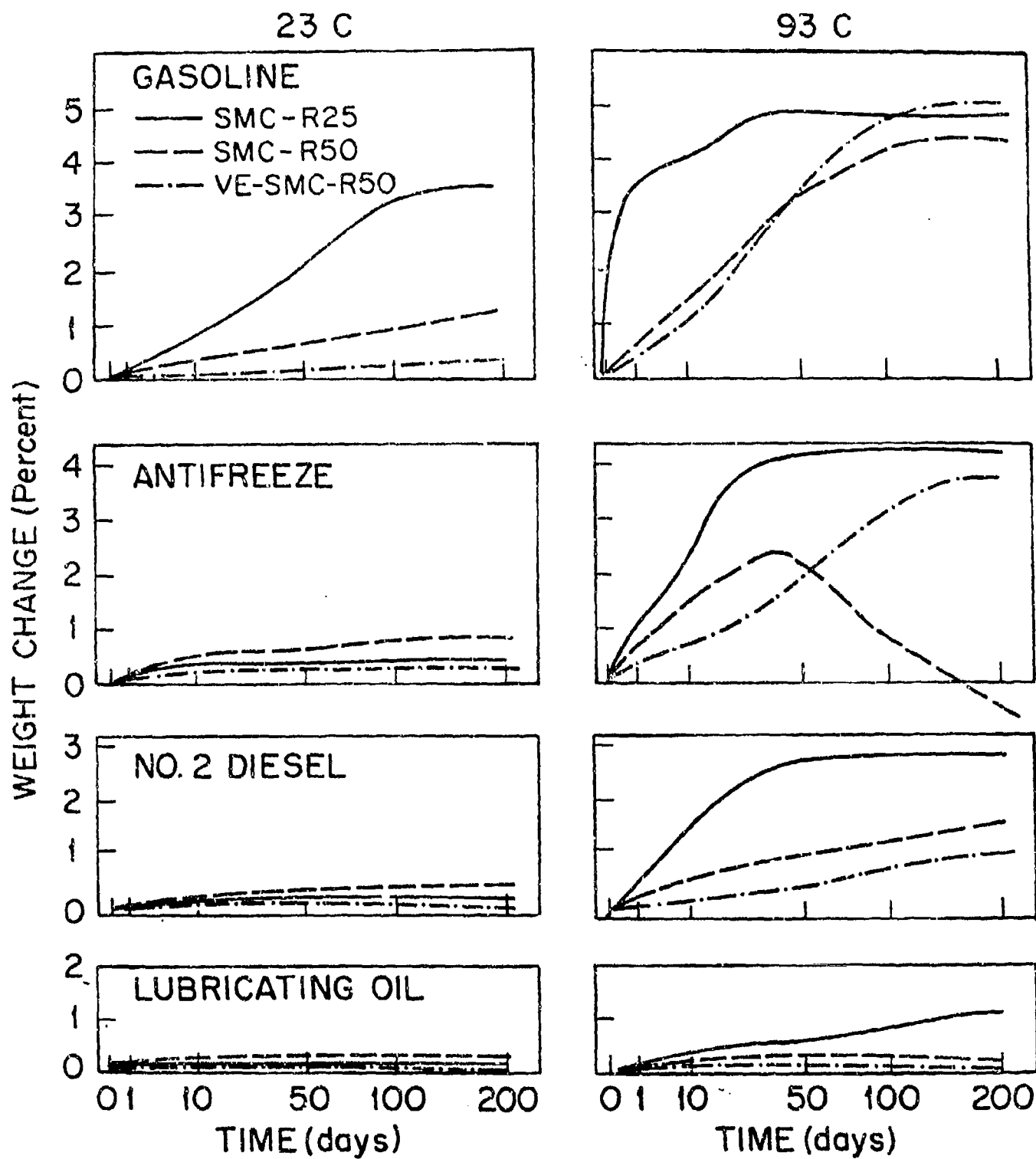


Figure 36: Weight change during immersion in different types of hydrocarbons
(refs. 4, 14)

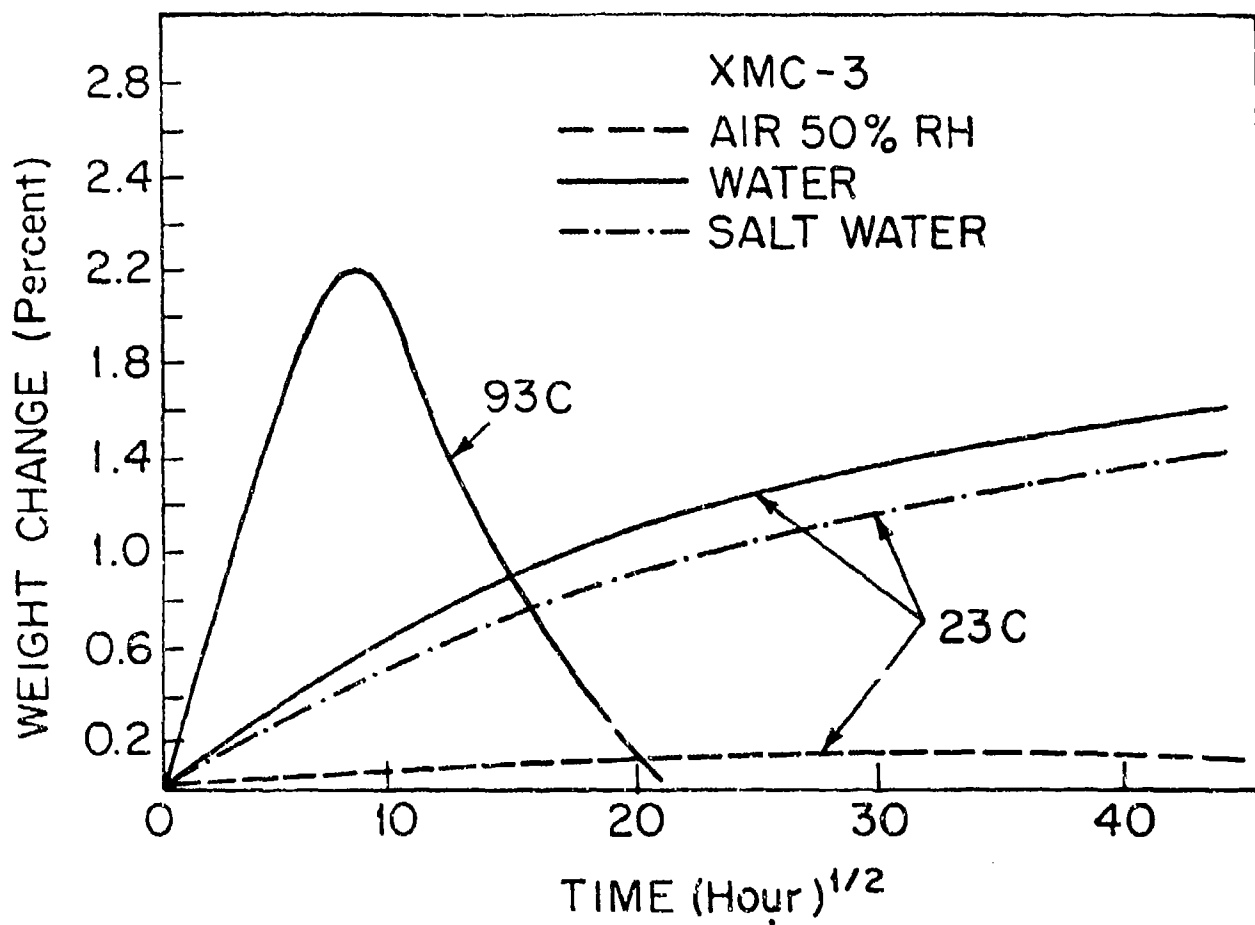


Figure 37: Weight change of XMC-3 immersed in humid air, water, and in 5% NaCl-water mixture (ref. 4)